



## Financial crises: Uncovering self-organized patterns and predicting stock markets instability

A. Spelta <sup>a,b</sup>, A. Flori <sup>c</sup>, N. Pecora <sup>d,\*</sup>, F. Pammolli <sup>b,c</sup>

<sup>a</sup> Dept. of Economics and Management, University of Pavia, Via San Felice al Monastero 5, 27100 Pavia, Italy

<sup>b</sup> Center for Analysis, Decisions, and Society (CADS) - Human Technopole, Milano, Italy

<sup>c</sup> Dept. of Management, Economics and Industrial Engineering, Politecnico di Milano, Via Lambruschini 4/B, 20156 Milano, Italy

<sup>d</sup> Dept. of Economics and Social Sciences, Catholic University, Via Emilia Parmense 84, 29122 Piacenza, Italy

### ARTICLE INFO

JEL codes:

C02  
C14  
C63  
G01

Keywords:

Complex systems  
Financial markets  
Herding behavior  
Early-warning indicator

### ABSTRACT

Financial markets are complex systems where investors interact using competing strategies that generate behaviours in which herding and positive feedbacks may lead to endogenous instabilities. This paper develops a novel methodology to detect the emergence of such phases by quantifying the intensity of self-organizing processes arising from stock returns' co-movements and self-similarities. Our methodology identifies a group of stocks, the Leading Temporal Module, whose statistical properties reflect the transition of the market into a crisis state. We define a topological indicator of the emergence of market discontinuity based on the autocovariance of the stocks in the Leading Temporal Module and on the ratio between the stocks' correlations within this group and the correlations between these stocks and those outside the leading module. This indicator provides early-warning market signals useful for policy-makers and investors by mapping the evolution of the topological properties of the leading module in different points in time.

### 1. Introduction

During the last two decades, financial markets have been characterized by an unprecedented level of interdependence and connectivity (see, e.g., [Gkillas, Tsagkanos, & Vortelinos, 2019](#); [Hausman & Johnston, 2014](#); [Vasconcelos & Ramirez, 2011](#)), generating complex phenomena, patterns and structures in the decision processes of market participants (see [Kirman, 2010](#)). Within this perspective, a strand of research has recently applied novel tools derived from statistical learning and statistical physics to deepen our understanding of the behaviour of financial markets and to solve problems arising in economics, finance and management science. In this respect, econophysics research has started to address the issue of quantifying and understanding large market fluctuations that may lead to financial crises (see, e.g., [Kutner et al., 2018](#); [Takayasu, Watanabe, & Takayasu, 2010](#)). This approach integrates different techniques and combines the top-down approach typical of financial economics with a bottom-up perspective for data analytics and forecasting, thus stimulating a complex systems science for financial markets that is under the spotlight of academic literature in finance and econophysics ([Ausloos, Ivanova, & Vandewalle, 2002](#);

[Ausloos, Jovanovic, & Schinckus, 2016](#); [Huber & Sornette, 2016](#); [Kutner et al., 2018](#); [Mantegna & Stanley, 1999](#); [Plerou, Gopikrishnan, Rosenow, Amaral, & Stanley, 2000](#)).

Against this background, periods of instability and crisis have been seen as generated by repeated, non linear, evolving interactions between investors' decisions ([Rosser, 1999](#); [Sornette, 2003, 2017](#)), i.e., waves of financial turmoil have been analyzed as self-organizing processes (see, e.g., [Hommes, 2013](#)). Interestingly, despite the spatial and temporal diversity of financial crises, some basic ingredients have been repeatedly found at the ground of different market crashes ([Sornette, 2017](#)). According to a recurring pattern, crises are in fact likely to begin with a successful bundle of sectors within the economy driven by apparently strong fundamentals, which foster credit expansion, money supply and, consequently, price growth. Then, more investors are drawn in by positive profit expectations, which may end in inducing the formation of a bubble, its expansion and, eventually, its burst. More generally, as it has been shown in the literature, the recurrent patterns leading to financial instability and turmoil are typically shaped by investors' herding behaviors ([Moon & Lu, 2015](#); [Preis, Schneider, & Stanley, 2011](#); [Scheffer et al., 2009](#); [Scheffer et al., 2012](#)) and positive feedback effects

\* Corresponding author.

E-mail addresses: [alessandro.spelta@unipv.it](mailto:alessandro.spelta@unipv.it) (A. Spelta), [andrea.flori@polimi.it](mailto:andrea.flori@polimi.it) (A. Flori), [nicolo.pecora@unicatt.it](mailto:nicolo.pecora@unicatt.it) (N. Pecora), [fabio.pammolli@polimi.it](mailto:fabio.pammolli@polimi.it) (F. Pammolli).

(Hommes, 2013; Lux, 1995, 1998), in which the dynamics of aggregate market variables are affected by individual expectations and vice-versa.

Forecasting the emergence of market transitions is thus of utmost importance for real world problems in many organizations, such as the design of macro-prudential policy interventions or portfolio allocation strategies. To be useful for policy and investment decisions, an indicator of market transitions should not only have statistical predictive power relying on real-time information, but it should also operate in a timely fashion. Signals provided by the indicator should arrive early enough so that policies and investment decisions can be effectively implemented, i.e., the indicator should provide early-warning signals (EWSs) of the dynamics of the underlying system.

Several methodologies have been proposed in the literature to investigate, for instance, how cross-market linkages, co-movements and inter-dependencies affect the sustainability conditions of evolving and complex financial environments (Andreou & Ghysels, 2009; Baillie & Bollerslev, 1994; Barberis, Shleifer, & Wurgler, 2005; Brenner & Kroner, 1995; Forbes & Chinn, 2004; Forbes & Rigobon, 2002; Gkillas et al., 2019). In particular, our investigation has been inspired by the biomedical research paper of Chen, Liu, Liu, Li, and Aihara (2012), who introduced the concepts of Dynamical Network Biomarkers (DNBs) to detect EWSs of the progression of complex diseases using throughput data.

In this paper, we establish an analogy between the identification of discontinuities in scientific and technological systems (Orsenigo, Pammolli, & Riccaboni, 2001; Pammolli & Riccaboni, 2002; Riccaboni & Pammolli, 2003; Pyka & Scharnhorst, 2009) and the early-warning detection of discontinuities in financial markets. In fact, we develop a synthetic topological indicator, which enables us to capture, parsimoniously, the emergence of shifts in the laws that rule the evolution of the system in time (see Chen et al., 2012). We propose to monitor the strengthening of the interactions and coordination among market participants as a signal for the emergence of an upcoming financial turmoil. As shown in Spelta, Pecora, Flori, and Pammolli (2018), during a pre-crisis stage, some general temporal and spatial properties hold: (i) a group of stocks<sup>1</sup> has an average *within* Pearson's Correlation Coefficient (PCC) that drastically increases in absolute value; (ii) the *between* average PCC of stocks in this group and any other stocks in the rest of the system greatly decreases in absolute value; (iii) the average autocovariance (AC) of stocks belonging to this group increases in absolute value. If the three above mentioned conditions are simultaneously satisfied, the corresponding group of stocks composes the Leading Temporal Module (LTM) of the system and its emergence can be seen as a signal of an upcoming increase of financial instability. In particular, we do interpret the increase of the autocovariance of stocks' returns as a sign of positive feedbacks (see Dakos et al., 2012; Lenton, Livina, Dakos, Van Nes, & Scheffer, 2012), while we hypothesize that herding behaviors empirically translate into an increasing correlation among stocks' returns (see Dakos et al., 2012; Hong & Stein, 2003; Lux, 1995).

Therefore, our paper aims at providing a rigorous investigation of the properties of the LTM sub-graph by connecting its emergence and evolution to specific behavioral attitudes of market participants. Indeed, other works (see e.g., Hommes, 2013; Sornette, 2003, 2017) have shown that in the presence of high expectations about the future price of an asset, the demand for that asset increases and the price becomes high as well, meaning that a large cumulative price movement may ensue leading the future value of the stock to increase its dependence on the current one (see Bao, Hennequin, Hommes, & Massaro, in press; Hommes, Sonnemans, Tuinstra, & Van de Velden, 2004; Hommes, Sonnemans, Tuinstra, & Van de Velden, 2008). Market crashes have been considered also as the consequence of herding behaviors emerging from the broken balance between investors' autonomous conducts and

the influence of their peers (see, e.g., Hirshleifer & Hong Teoh, 2003; Hwang & Salmon, 2004; Preis et al., 2011), thus implying that investments strategies face a higher interconnectivity prior and during a financial crash with respect to "business as usual" days.

More specifically, we rely on the temporal and spatial properties of the LTM to build an aggregate and flexible indicator, which we employ to detect the emergence of significant changes in financial markets. In particular, we aim at predicting distress phases on aggregate indices, which represent markets as a whole, through the investigation of the dynamical behavior of the sub-graph of the LTM members. To assess the validity of our approach, we exploit data from different geographical areas and covering various crisis episodes. We refer to the US, Europe and Asia-Pacific stock markets during the period 2005–2018 in a way that both major global financial crisis and different local critical events are mapped. We show that when we monitor autocovariance we succeed in timely anticipate market distress and we outperform other early-warning indicators of phase transitions in complex systems such as the one related to Chen et al. (2012). The results of the present paper also extend preliminary findings reported in Spelta, Pecora, et al. (2018), by revealing within an applied framework the usefulness of our indicator for both policy-makers and investors. In fact, from a policy-maker viewpoint the indicator can help in taking policy decisions such as the timely activation of macro-prudential policies, while from an investor perspective we show how the ability of the indicator to correctly anticipate changes in the aggregate stock price indices and, in particular, around large market movements can be exploited to build a simple investment strategy.

A distinguishing feature of our analysis is the great emphasis we pose on the feedback mechanisms between assets returns and the behavior of market participants. The proposed indicator we come up to considers the strengthening of interconnections among financial assets as a marker of a turning point of a financial cycle in the run-up of a financial crisis. Our findings reveal that the identification and evolution of the LTM sub-graph can be a relevant and flexible tool for macro-prudential policies and portfolio allocations, hence a useful practical approach for adaptive systems and organization contexts which embrace complexity science for business research and innovation policy (Ahrweiler, Gilbert, & Pyka, 2016; Carpenter, Li, & Jiang, 2012; Roundy, Bradshaw, & Brockman, 2018; Slotte-Kock & Coviello, 2010).

The paper proceeds as follow: in Section 2 we describe the data we employ and we present the methodology underlying the construction of our indicator. In Section 3 we report the results of the application of our methodology in different markets. We evaluate the usefulness of our early-warning indicator from a policymaker perspective and we also illustrate an investment strategy based on the early-warning signals provided by our indicator. Section 5 concludes. For the sake of readability Appendix A reports the list of symbols and the corresponding definitions used through the paper.

## 2. Materials and methods

The dynamic of the LTM members defines the evolution of the underlying system since stocks belonging to that module are the first movers that drive the whole system into a phase transition (see Spelta, Pecora, et al., 2018). By construction, the LTM members are highly and dynamically correlated in the pre-crisis period and thus, they are expected to form a strongly connected component from a network theory viewpoint.

We develop our early-warning indicator to assess the proximity of a market crash by following a network theory perspective (see, e.g., Borgatti & Halgin, 2011; Newman, 2003; Wang & Chen, 2003, among others). The financial system is represented as a dynamical temporal graph  $G_t = (N_t, E_t)$  with the set of nodes  $N_t$  being the stocks of the selected market, and the set of edges  $E_t$  representing the pairwise correlations ( $PCC(z_i(t), z_j(t))$ ) between each pair of stocks' returns ( $z_i(t), z_j(t)$ ) computed over a given moving window. In general, we establish a

<sup>1</sup> In the present work, stocks, assets and financial instruments are used as synonyms.

procedure to split these stocks into two groups or communities: (i) the set of stocks  $N_t^{LTM}$  composing the LTM, and (ii) the remaining financial instruments  $N_t^o = N_t \setminus N_t^{LTM}$  outside the leading module. If the networked system is approaching a phase transition, we observe that: (i) the autocovariance of the returns time series of the  $N_t^{LTM}$  members increases in absolute terms; (ii) the absolute value of the correlation between stocks in  $N_t^{LTM}$  also increases; (iii) conversely, the absolute value of the correlation between a stock in  $N_t^{LTM}$  and another stock in  $N_t^o$  decreases to zero.

To characterize the evolution of the system, we synthesize the statistical properties reported above by proposing an early-warning indicator. This is done in line with contributions proposed in other socio-economic and biological contexts (see e.g., Oya, Aihara, & Hirata, 2014; Liu, Chen, Aihara, & Chen, 2015; Moon & Lu, 2015). More precisely, in accordance to Li, Zeng, Liu, and Chen (2013), we develop a procedure for detecting the LTM at each time  $t$  (Appendix B shows the pseudo-code for extracting the LTM sub-graph and the corresponding early-warning indicator). Starting from the  $N \times T$  matrix containing the adjusted closure prices of  $N$  stocks for  $T$  reporting days, the log-returns are computed. Then, a sub-matrix of the returns (obtained using a rolling window of  $w$  working days) is extracted for calculating stocks' autocovariance at each time  $t$ . Stocks are then sorted in descending order according to their autocovariance values ( $AC_t$ ), and only the highest  $x$ -percent of them are included in the clustering procedure. This step allows us to have a group  $N_1$  of stocks with the highest autocovariance at period  $t$ . These stocks are then grouped together, using as a clustering measure the average correlation of their returns between periods  $t-w$  and  $t$ . The Silhouette<sup>2</sup> value is then employed to determine the optimal number of clusters. To compute the early-warning indicator, for each cluster  $H$  we calculate the *within* absolute average correlation ( $<|PCC_t^H|>$ ) and the *between* absolute average correlation ( $<|PCC_t^{N_1 \setminus H}|>$ ), together with the absolute average autocovariance value  $<|AC_t^H|>$ . By doing this, we end up with  $I_t^{AC,H} = \frac{<|AC_t^H|><|PCC_t^H|>}{<|PCC_t^{N_1 \setminus H}|>}$  for each cluster. Finally, the LTM at time  $t$  is the subset of financial instruments that presents the maximum value<sup>3</sup> of  $I_t^{AC,H}$ , i.e.:

$$I_t^{AC} = \max \{ I_t^{AC,H} \} \quad (1)$$

To inspect whether our proposed indicator is able to identify a distress in stock markets, we employ standard approaches from crisis signaling. Generally speaking, early-warning models attempt to differentiate between vulnerable (i.e., pre-crisis and crisis) and tranquil states. In practice, we aim at separating vulnerable and tranquil classes of observations by estimating the probability of being in a vulnerable state. In our approach, to assess the performance of the indicator, we conduct recursive out-of-sample tests, meaning that for each day we use only the information available up to that time point to produce forecasts. By using the information in a realistic manner, we basically test whether our indicator has an ex-ante power for predicting crisis events. Following a standard evaluation framework for early-warning models, we aim at mimicking an ideal leading indicator  $L \in \{0, 1\}$ , which is a

<sup>2</sup> The Silhouette value measures how similar a stock is to other stocks in its own cluster, when compared to stocks in other clusters. A high Silhouette value signals that a stock is well-matched to its own cluster while it is poorly-matched to neighbor clusters.

<sup>3</sup> Spelta, Pecora, et al., 2018 performed several robustness checks on the parameters  $w$  (this parameter represents the length of the moving window employed to compute the correlations) and  $x$  (this parameter represents the percentage of stocks selected for the clustering procedure) showing the relationships between changes in the behavior of the indicator and in the parameters values. In particular  $w$  goes from 10 days to a working month while the parameter  $x$  takes values that vary from 100 to 40 percent as a robustness check.

Predicted Class	Actual Class	
	Pre-crisis period	Tranquil period
Signal	Correct call <i>True Positive</i> (TP)	False alarm <i>False Positive</i> (FP)
No Signal	Missed crisis <i>False Negative</i> (FN)	Correct silence <i>True Negative</i> (TN)

Fig. 1. Contingency matrix. The matrix reports the four cases defining the correct or wrong crisis identification.

binary variable assuming value one in vulnerable periods and zero otherwise. In practice, to detect events in  $L$ , we need a continuous measure indicating membership in a vulnerable state  $p \in [0, 1]$ , which is then turned into a binary prediction  $B$  that takes the value one if  $p$  exceeds a specified threshold  $\tau \in [0, 1]$  and zero otherwise. The correspondence between the predictions in  $B$  and the ideal leading indicator  $L$  can then be summarized into the so-called contingency matrix, as described in Fig. 1.

For evaluating the predictive performance, we then compute some standard measures employed in the machine learning literature (see Provost & Kohavi, 1998). In particular, we calculate the area under the Receiver Operating Characteristic curve (namely, the AUROC) and the area under the Precision-Recall curve (namely, the AUPR). The Receiver Operating Characteristic (namely, the ROC) curves plot the false positive rate (namely, the FPR) against the true positive rate (namely, the TPR). To be more explicit:

$$FPR = \frac{FP}{FP + TN} \text{ and } TPR = \frac{TP}{TP + FN}$$

In addition, the PR curves plot precision (P) versus the recall (R), or, more explicitly:

$$P = \frac{TP}{TP + FP} \text{ and } R = TPR = \frac{TP}{TP + FN}$$

where  $TP, TN, FP$  and  $FN$  stand for true positive, true negative, false positive and false negative (see Fig. 1), respectively. Notice that, while the definition of true positive rate and recall is the same, the two curves differ for the quantity plotted against these values. Namely, the false positive rate in the first case and the precision in the second case.

For an early-warning model, we need two types of data: crisis events and vulnerability indicators. Accordingly, we introduce two definitions of crisis events. The first occurs if the drop in the returns of the aggregate market index is at least 3% and, in that case, we assume the ideal leading indicator  $L$  takes value one from the dropping date to the entire previous month. The second case considers a -4% drop in the aggregate market index returns and assigns a value of one to  $L$  at each day of the previous month; however, in this case the value one is assigned only to one day per time, on a day-by-day basis. In this way we can investigate the predictive power of the early-warning indicator in terms of its capability to anticipate crisis events, i.e., we can evaluate the persistence of the AUROC/AUPR values as long as we seek to anticipate a crisis event on a wider time horizon. In both cases, the selected values represent extreme events that lie in the first or second percentiles of the returns distributions (see Fig. 2). These thresholds have been typically used, for instance, for risk management purposes (see Kuester, Mitnik, & Paolella, 2006).

As concerns the vulnerability signals, we compare our indicator  $I_t^{AC}$

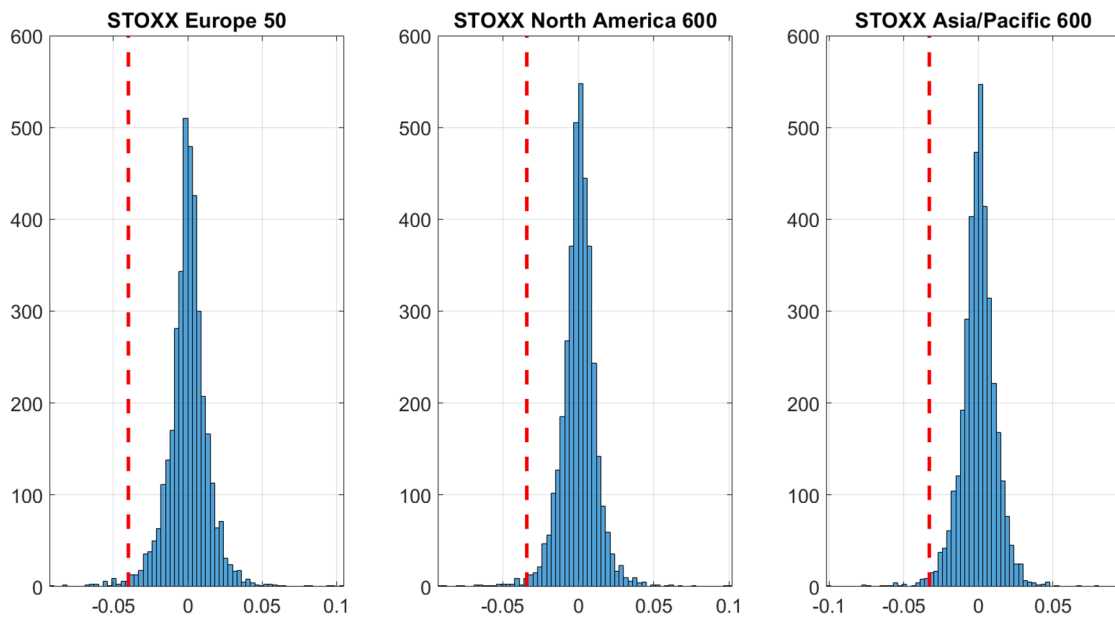


**Fig. 2.** Return distributions along with the first percentile indicating crisis thresholds. The three panels represent the return distributions of the aggregate indices while the dashed red lines indicate the first percentile. This threshold has been used as a reference point for crisis occurrences along the empirical analysis. In particular the left panel refers to Europe, the central panel to the North America and the right panel to the Asia/Pacific region.

with other measures, such as the method proposed by [Chen et al. \(2012\)](#), denoted by  $I^{STD}$ , and an indicator constructed by mixing both standard deviation ( $STD$ ) and autocovariance ( $AC$ ) values. In particular, following the same clustering procedure described above we end up with

$$I_t^{AC,STD,H} = \frac{<|AC_t^H| ><|STD_t^H| ><|PCC_t^H| >}{<|PCC_t^{N_1 \setminus H}| >},$$

for which we select

$$I_t^{AC,STD} = \max\{I_t^{AC,STD,H}\}. \quad (2)$$

Additionally, we report the findings for the original indicator and its smoothed version, obtained by using a second order polynomial in a locally estimated scatterplot smoothing (LOESS).

One of the main goals of the present paper is to evaluate to what extent our indicator is useful for a policymaker. Against this background, [Kaminsky and Reinhart \(1999\)](#) and the literature following their seminal contribution propose to measure the usefulness of an early-warning indicator by computing the adjusted noise-to-signal ratio. A useful indicator is supposed to have a noise-to-signal ratio less than one. This criterion, although being a necessary condition for a useful indicator, could result in errors that are unacceptable to policymakers given their preferences. Moreover, it does not quantify the gain associated with receiving signals from an indicator as compared to ignoring it, which also depends on users' preferences.

Therefore, we follow [Sarlin \(2013\)](#) to design a policymaker loss-function by adopting the concepts of absolute and relative usefulness as measures of classification performance. The loss-function is based on three ingredients: the error types, the policymakers' preference between error types and the probabilities of being in crises or in tranquil periods. The type I error is defined as the ratio of missed crises over the total number of crisis events, i.e.,  $T_1 = FN/(FN + TP)$ , while the type II error is the proportion of false alarms to the number of tranquil periods, i.e.,  $T_2 = FP/(TN + FP)$ . The parameter  $\mu$  defines the policymakers' relative preference between type I and II errors. Finally, we define the unconditional probabilities of crises as  $P_1$  and of tranquil periods as  $P_2$ . These variables take into account potential differences in the amount of the two classes. Based on these values, we exploit the following loss function:

$$Lo(\mu) = \mu T_1 P_1 + (1 - \mu) T_2 P_2. \quad (3)$$

According to this loss function, the absolute usefulness of the prediction can be therefore computed by comparing the forecast obtained from the indicator to that of a naive guess made by a policymaker that assumes to always or never signaling depending on the class frequency and preferences, namely:

$$U_a(\mu) = \min(\mu P_1, (1 - \mu) P_2) - Lo(\mu). \quad (4)$$

Notice that, in principle, a negative absolute usefulness can arise when the indicator performs so poorly that a policymaker that always signals the high-frequency class outperforms the EWS. Additionally, we also employ the relative usefulness, i.e.  $U_r$ , to compare the absolute usefulness provided by our indicator to the absolute usefulness of a perfect model ( $Lo(\mu) = 0$ ):

$$U_r(\mu) = \frac{U_a(\mu)}{\min(\mu P_1, (1 - \mu) P_2)}. \quad (5)$$

## 2.1. Data

In order to prove the efficacy of the early-warning indicator under different market settings and conditions, we test the methodology on the returns computed on the daily closure prices of three different markets (North America, Europe and Asia/Pacific). We approximately refer to stocks related to the STOXX Ltd. indices, which are commonly used to design a wide range of investment products such as Exchange Traded Funds (ETFs), Futures and Options, and structured products.<sup>4</sup> These datasets are very heterogeneous, being composed by a different number of stocks regarding different geographical areas and being affected by different types of crises (e.g., the sub-prime financial crisis and the European sovereign debt crisis). The first dataset we consider includes stocks referring to the STOXX North America 600 Index, a broad yet liquid subset of the STOXX Global 1800 Index with a fixed number of 600 components from US and Canada. The STOXX North America 600 includes the largest companies in the North America region. The second

<sup>4</sup> For details, see: <https://www.stoxx.com/>.

**Table 1**

Summary Statistics. Summary statistics of the reference stocks markets (proxies for STOXX North America 600, STOXX Europe 50 and STOXX Asia/Pacific 600) divided into three sub-periods, namely 2005–07, 2007–13 and 2013–18. For each index and sub-period, we report the minimum (min.), the maximum (max.), the average (mean) values of the daily returns along with the standard deviation (std.), the skewness (skew.), and the kurtosis (kurt.).

Period	STOXX North America		STOXX Europe 50		STOXX Asia/Pacific	
	600			600		
	min.	max.	min.	max.	min.	max.
2005–07	−0.1032	0.0860	−0.0243	0.0263	−0.0833	0.0866
2007–13	−0.1357	0.1068	−0.0447	0.0405	−0.1206	0.1016
2013–18	−0.0990	0.0885	−0.0292	0.0290	−0.0880	0.0862
	mean	std.	mean	std.	mean	std.
2005–07	0.0004	0.0150	0.0005	0.0092	0.0007	0.0165
2007–13	−0.0001	0.0194	−0.0003	0.0157	−0.0004	0.0202
2013–18	0.0004	0.0140	0.0002	0.0106	0.0004	0.0155
	skew.	kurt.	skew.	kurt.	skew.	kurt.
2005–07	−0.0197	23.539	0.1008	5.5671	0.2769	11.202
2007–13	0.0194	26.322	−0.0888	5.6234	−0.1490	16.609
2013–18	0.0140	27.643	−0.0326	5.7625	0.0149	15.525

dataset is represented by stocks referring to the STOXX Europe 50 Index that provides a representation of supersector leaders in Europe. The STOXX Europe 50 covers stocks from 17 European countries, namely: Austria, Belgium, Czech Republic, Denmark, Finland, France, Germany, Ireland, Italy, Luxembourg, the Netherlands, Norway, Portugal, Spain, Sweden, Switzerland and the United Kingdom. The third group includes stocks referring to the STOXX Asia/Pacific 600 Index that encompasses, basically, the largest companies in Australia, Hong Kong, Japan, New Zealand and Singapore. All the data have a daily frequency and range from 2005 to 2018.

**Table 1** provides some summary statistics for the three markets. We refer to the stocks composing each index separately for three time intervals referring to the prior-crisis period (2005–07), the crisis (2007–13), and the post-crisis period (2013–18). The length of the crisis interval is set according to the economic and financial events which have affected the global capital markets, such as the 2007–08 financial crisis and the 2011–12 European sovereign debt crisis. **Table 1** reports the minimum, the maximum, the mean, the standard deviation, the skewness, and the kurtosis of the distribution of the daily returns. We note that during the crisis, average returns are negative in each of the three stock markets and the standard deviations indicate high volatility, in line also with the minimum and maximum values of the returns distributions. Moreover, we observe that the descriptive statistics for prior

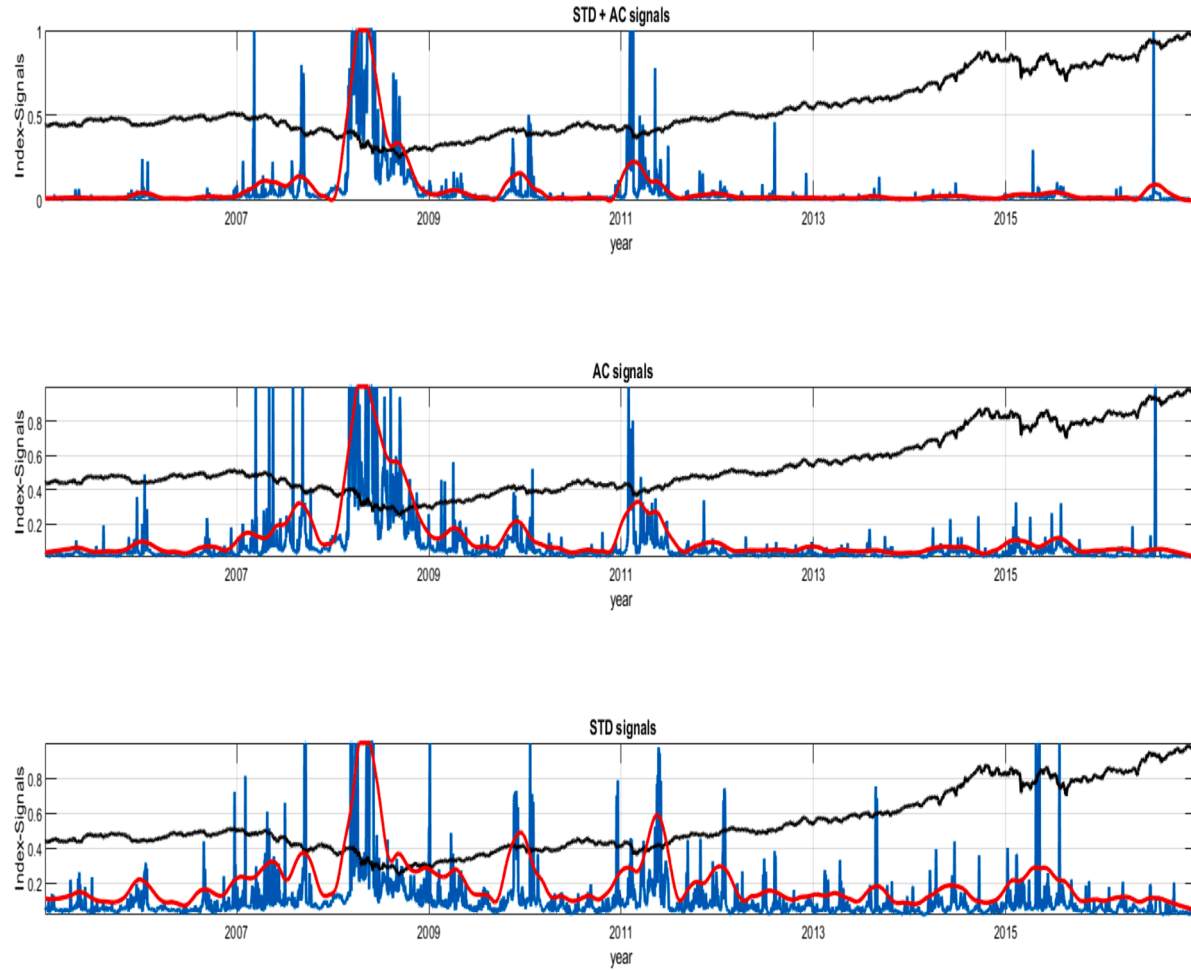


**Fig. 3.** Early-warning indicator patterns and the underlying aggregate index dynamic. Stock market: North America. The three panels represent the original early-warning indicators (blue), together with the smoothed ones (red) and the STOXX North America 600 aggregate index (black). The upper panel refers to the signal produced by using autocovariance and standard deviation  $I_t^{AC,STD}$ , together with the PCC. The central panel encompasses our proposed indicator that, beside the PCC, relies only on autocovariance. The lower panel refers to the original indicator  $I_t^{STD}$  proposed by Chen et al. (2012). In particular, the label STD+AC refers to the mixed signal  $I_t^{AC,STD}$ , AC denotes our early-warning indicator  $I_t^{AC}$  and finally STD refers to the  $I_t^{STD}$ . (For interpretation of the references to colour in this figure legend, the reader is referred to the web version of this article.)

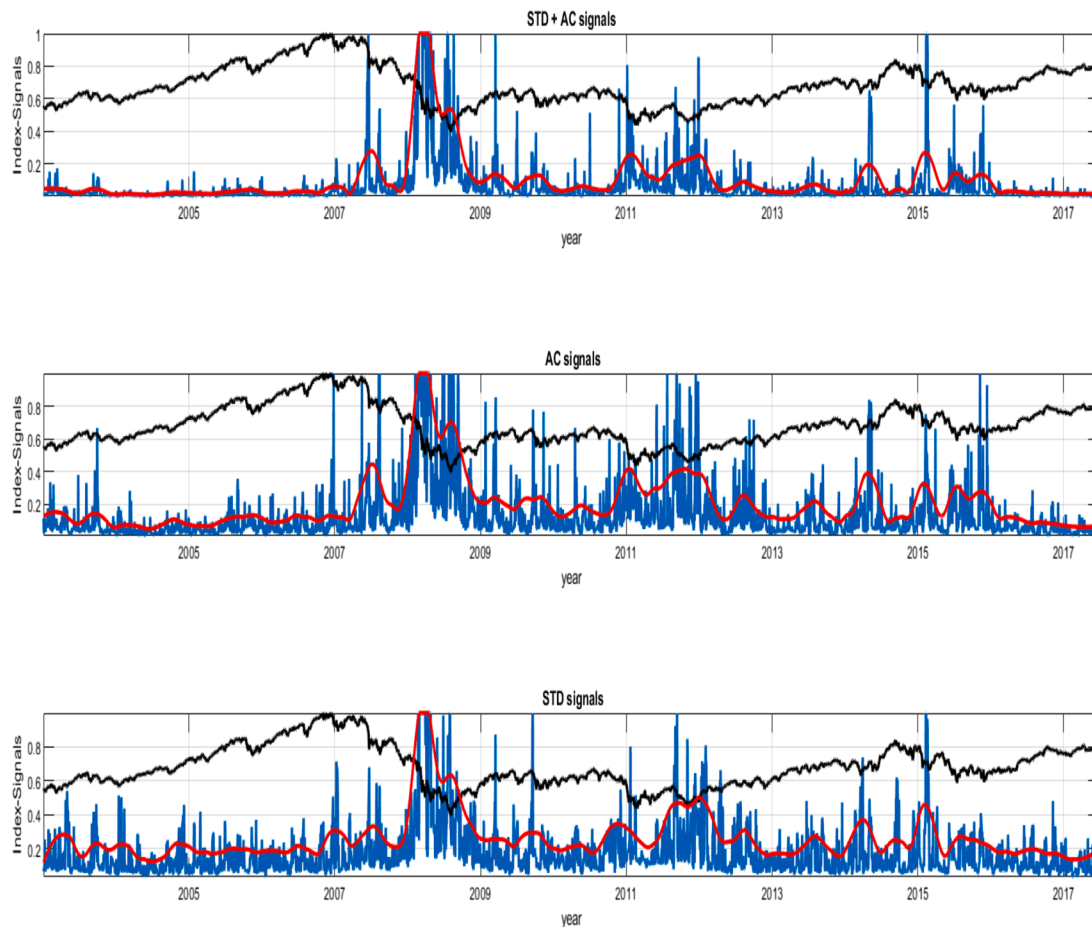


**Fig. 4.** Early-warning indicator patterns and the underlying aggregate index dynamic. Stock market: Europe. The three panels represent the original early-warning indicators (blue), together with the smoothed ones (red) and the STOXX Europe 50 aggregate index (black). The upper panel refers to the signal produced by using autocovariance and standard deviation  $I_t^{AC,STD}$ , together with the PCC. The central panel encompasses our proposed indicator that, beside the PCC, relies only on autocovariance. The lower panel refers to the original indicator  $I_t^{STD}$  proposed by Chen et al. (2012). In particular, the label STD+AC refers to the mixed signal  $I_t^{AC,STD}$ , AC denotes our early-warning indicator  $I_t^{AC}$  and finally STD refers to the  $I_t^{STD}$ . (For interpretation of the references to colour in this figure legend, the reader is referred to the web version of this article.)

and post crisis periods are slightly different, revealing that the turbulence of the crisis still affects the subsequent years in a way that markets do not completely retrieve the pre-crisis configuration.

### 3. Results

For each of the three datasets, we consider the aggregate market index and its stock constituents. We focus on anticipating the dynamics of the aggregate index starting from the interactive behavior of its underlying components which emerges from the study of the LTM. In Figs. 3–5 we show the signals generated by the three alternative indicators discussed in Section 2 for the North America, Europe and Asia/Pacific stock markets, respectively. In all the figures, the blue lines represent the indicators  $I_t^{AC}$ ,  $I_t^{STD}$ , and  $I_t^{AC,STD}$ , the red lines are the corresponding smoothed versions of these indicators, while black lines refer to the corresponding market indices. To facilitate comparisons across early-warning signals, each series has been normalized.

We assess the early-warning performances of the proposed indicators along different market phases by studying the dynamics of these indicators against the respective aggregate market indices. In particular, we attempt at anticipating the most relevant episodes of market distress by looking at the dynamics of the early-warning indicators compared with the market course of the corresponding underlying index.

Notice that all the three indicators behave in a fairly similar way. However, evidences provided by the smoothed versions indicate that  $I_t^{AC}$

and the mixed indicator  $I_t^{AC,STD}$  better discriminate between crises and business as usual days than  $I_t^{STD}$ . Indeed,  $I_t^{AC}$  and  $I_t^{AC,STD}$  assume low values in correspondence of tranquil phases, while they show a sharp rise during crisis times. By contrast, the indicator proposed by Chen et al. (2012) (i.e.,  $I_t^{STD}$ ) seems less prone to generate signals able to timely distinguish between bad and good market phases.

The predictability performance of our proposed indicator relates to the behavioral features embedded in its mathematical formulation. Indeed, during a phase of market distress, the rise of  $I_t^{AC}$  reflects the increase of both the autocovariance and the correlation between the market dynamics of the LTM members. Economically, this upward pattern occurring during distressed periods reveals the interdependences between herding behaviors and positive feedbacks, which typically manifest more frequently in such market phases (see, e.g., Shiller & Pound, 1989). In behavioural economics, indeed, phenomena such as imitation, herding behaviors and positive feedbacks have been shown as key factors leading to endogenous instabilities (Hüsler, Sornette, & Hommes, 2013; Zhao et al., 2011). Positive feedbacks and herding behaviors may foster, for instance, the accumulation of instability and drive the underlying market into new configurations (Flori, Pammolli, Buldyrev, Regis, & Stanley, 2019; Schweitzer et al., 2009; Sornette, 2002, 2003; Spelta, Flori, & Pammolli, 2018). This occurs due to the behaviour of the investors, who are likely to coordinate on similar allocation strategies (see Hommes et al., 2004). A possible

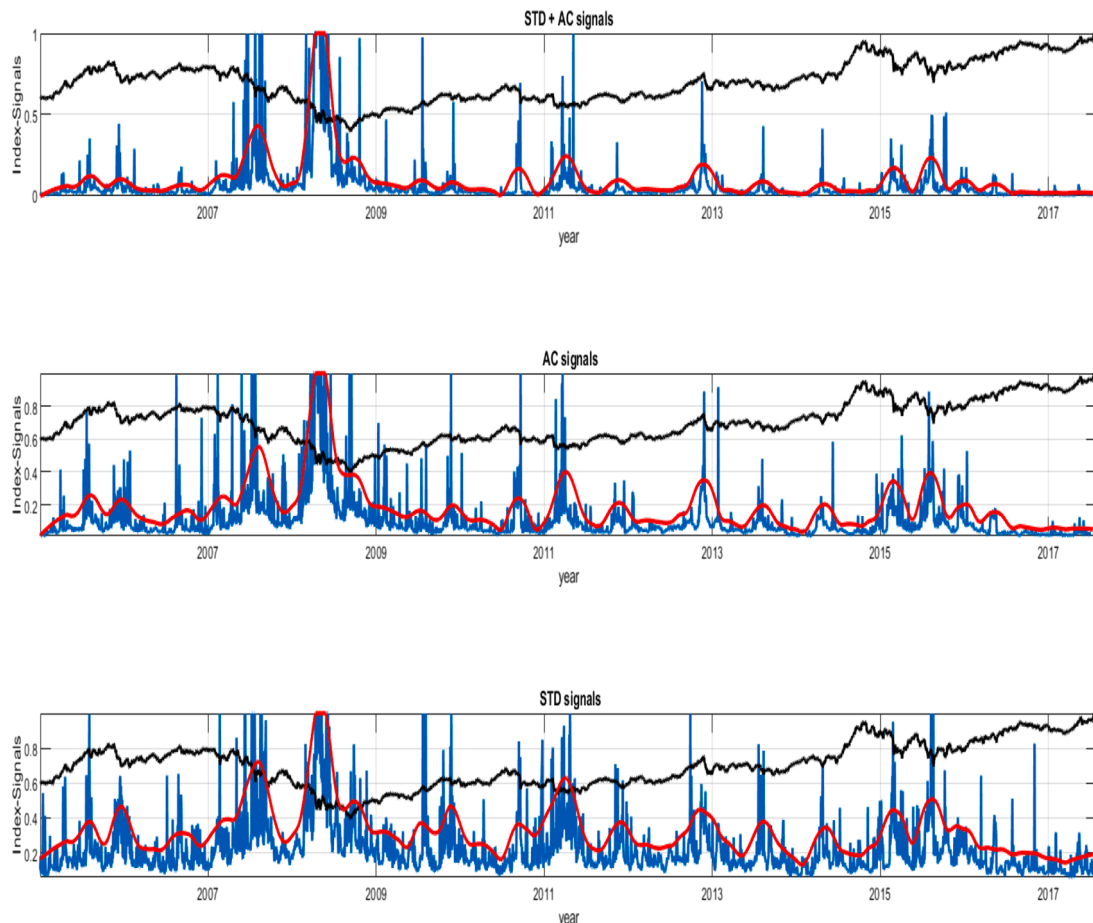


**Fig. 5.** Early-warning indicator patterns and the underlying aggregate index dynamic. Stock market: Asia/Pacific. The three panels represent the original early-warning indicators (blue), together with the smoothed ones (red) and the STOXX Asia/Pacific 600 aggregate index (black). The upper panel refers to the signal produced by using autocovariance and standard deviation  $I_t^{AC,STD}$ , together with the PCC. The central panel encompasses our proposed indicator that, beside the PCC, relies only on autocovariance. The lower panel refers to the original indicator  $I_t^{STD}$  proposed by Chen et al. (2012). In particular, the label STD+AC refers to the mixed signal  $I_t^{AC,STD}$ , AC denotes our early-warning indicator  $I_t^{AC}$  and finally STD refers to the  $I_t^{STD}$ . (For interpretation of the references to colour in this figure legend, the reader is referred to the web version of this article.)

intuition for the emergence of such characteristics can be the following one: suppose there is a sequence of days when investors receive certain trading signals, which stimulate trading intensity and, as consequence, more price volatility that favors herding-induced coordination among investors' behaviours. Under these circumstances, an unexpected negative shock can foster the onset of a turbulent period since investors are likely to reverse their investment strategies in a similar fashion. This coordinated market practice maps into the growing value assumed by our early warning indicator, since these market conditions stimulate a rise in the autocovariance and in the correlation of the LTM stocks' returns. Conversely, it may also be the case that, even in a turbulent period, there may be days in which investors receive weak trading signals, which lead volatility to decline. Accordingly, herding-induced coordination dissolves and a calm period emerges, with a consequent decline in the values of  $I_t^{AC}$ .

To provide a quantitative assessment about the predictive power of the three proposed early-warning indicators, we analyze the area under the ROC curve (i.e., AUROC) computed for different moving windows  $w$  and for several time steps referring to the leading indicator  $L$ . More specifically, the ROC curve is a pairwise plot showing true and false positive rates for various classification thresholds, which is thus an approach not tied to a predetermined loss function but it is a map reporting the entire space of trade-offs for a given classification problem. To measure the overall classification ability of the indicators, a synthesis

of all the trade-offs contained in the ROC curve is provided by AUROC values. Notice that a perfect classifier has  $AUROC = 1$ , whereas 0.5 for a purely random classifier. Additionally, the AUROC asymptotic distribution is Gaussian under general conditions (see Berge & Jordà, 2011), meaning that we can easily construct inference and comparisons between different classifiers. Despite the fact that this approach has been firstly adopted in other scientific fields such as radar signal, medicine and machine learning (see, e.g., Lusted, 1960; Peterson & Birdsall, 1953; Spackman, 1989; Swets, 1973), nowadays it is widely employed also in economics. For instance, similar machine learning diagnostics are applied by Khandani, Kim, and Lo (2010) in the context of consumer credit risk, by Berge and Jordà (2011) for discriminating between expansions and recessions phases of the business cycle, and by Alessi and Detken (2011) for detecting early-warning indicators of boom and bust cycles.

Figs. 6 and 7 show that, as expected, all the indicators provide better early-warning signals in the proximity of crisis periods, while the persistence of the AUROC values decreases as long as we seek to anticipate a market crisis with a wider time horizon. Additionally, these figures provide also evidence that our indicator, together with the mixed signal, outperforms the EWS proposed by Chen et al. (2012), i.e.  $I_t^{STD}$ , thus providing more informative signals regarding the current state. In particular, for the  $-4\%$  crisis scenario,  $I_t^{STD}$  produces AUROC values in line with the other two indicators (near 80%) up to one week before the

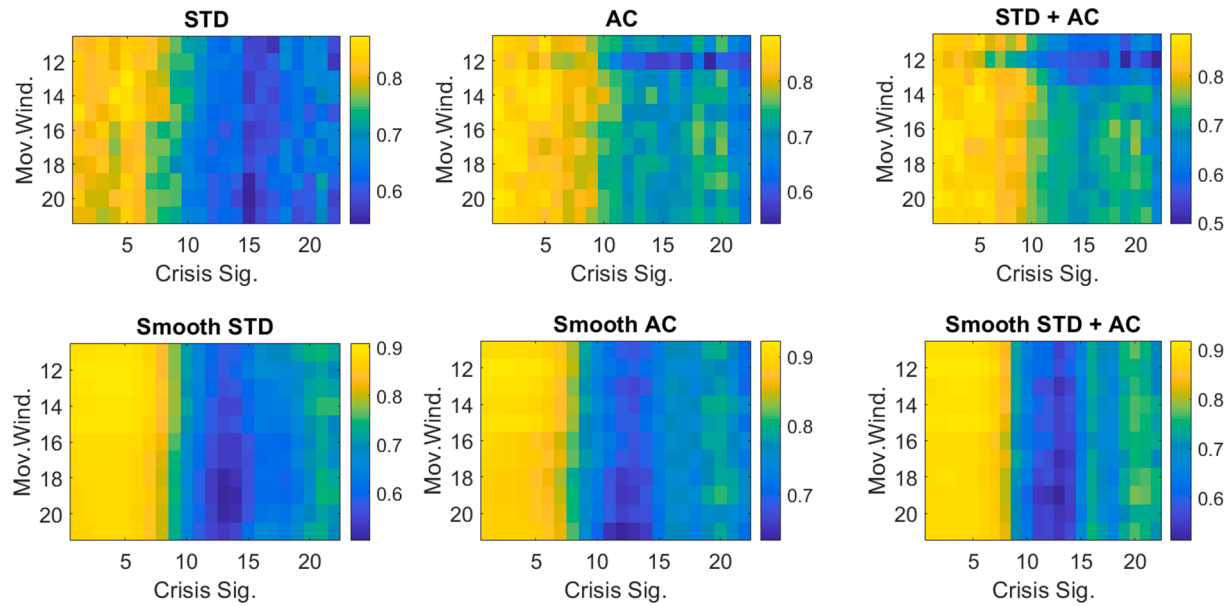


**Fig. 6.** AUROC values for different moving windows. Stock market: North America. Each plot represents the AUROC obtained by varying the moving window  $w$  used to compute the indicators. The colors refer to the AUROC values related to the  $-4\%$  crisis scenario in which, beside the different windows (reported on the y-axis), we also consider varying time steps for the leading indicator  $L$  (reported on the x-axis).  $L$  takes value 1 gradually, one day at a time, up to one month behind the crisis event. The upper panels represent the results related to the original early-warning indicators while the bottom ones encompass results obtained for the smoothed signals. The different columns represent the results obtained for  $I_t^{STD}$ ,  $I_t^{AC}$  and  $I_t^{AC,STD}$ , respectively.

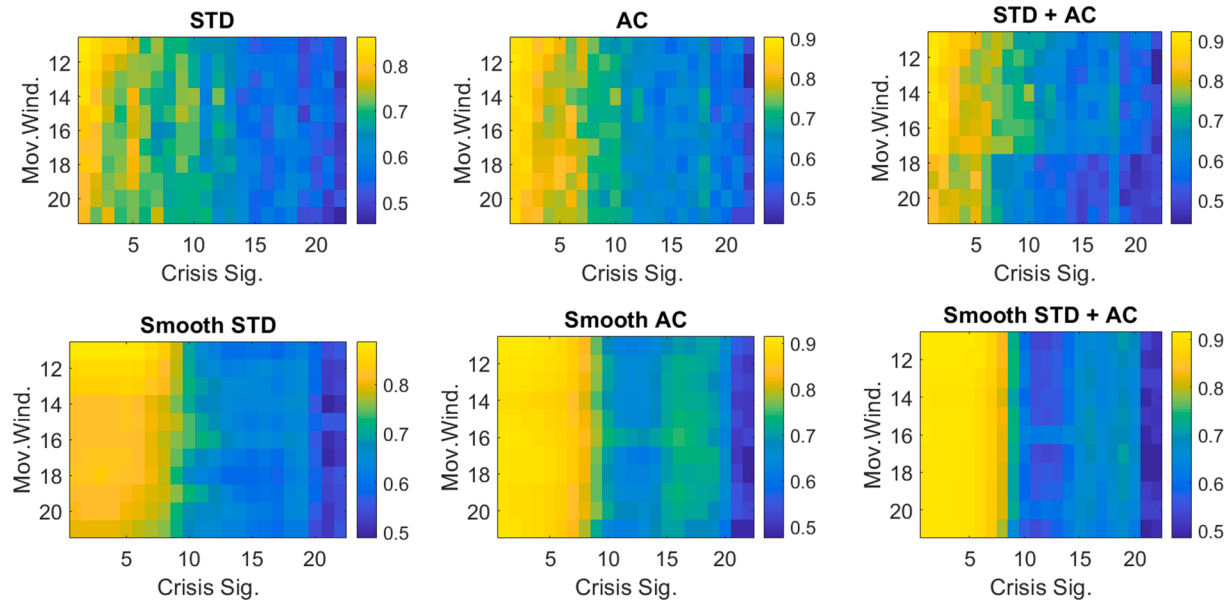


**Fig. 7.** AUROC values for different moving windows. Stock market: Europe. Each plot represents the AUROC obtained by varying the moving window  $w$  used to compute the indicators. The colors refer to the AUROC values related to the  $-4\%$  crisis scenario in which, beside the different windows (reported on the y-axis), we also consider varying time steps for the leading indicator  $L$  (reported on the x-axis).  $L$  takes value 1 gradually, day by day, up to one month behind. The upper panels represent the original indicators while the bottom ones encompass the results obtained for the smoothed indicators. The different columns represent the results obtained for  $I_t^{STD}$ ,  $I_t^{AC}$  and  $I_t^{AC,STD}$ , respectively.

event, but then it shows a decreasing performance, while  $I_t^{AC}$  and  $I_t^{AC,STD}$  tend to remain higher, approximately near 70%, up to a working month in the case of North America and near 60% in the case of Europe and Asia/Pacific stock markets. Notice also that all the three indicators provide AUROC values greater than 0.5, meaning that they embed useful information for crisis signaling since they have a higher performance with respect to a naive indicator. Moreover, Appendix C reports some robustness check to show the sensitivity of these findings to changes in

the value of the parameter  $x$  together with the results referring to the area under the PR curve.

An additional assessment for the validation of the performance of our crisis indicator involves the comparison of our EWS with three additional alternatives. Namely we compare  $I^{AC}$  against volatility indices such as the CBOE Volatility Index (Vix), the Crude Oil Volatility Index (Ovx) and the Geopolitical Risk indicator (Gpr). The Vix is a real-time market index representing market's expectation of 30-day forward-looking volatility. It provides a measure of market risk and investors'

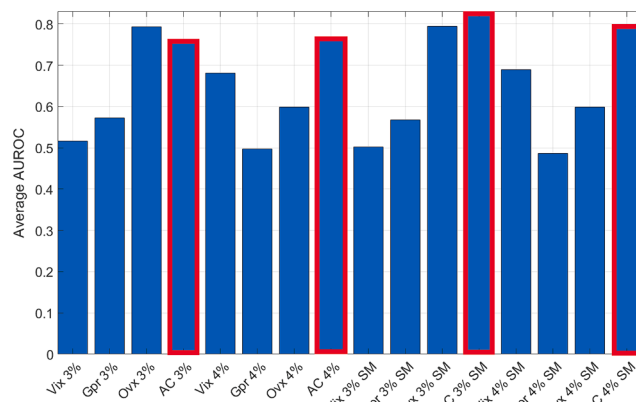


**Fig. 9.** Comparison of the AUROC values for the North America index. The blue bars represent the average AUROC values obtained with the Vix, the Gpr and the Ovx indices, along with the AUROC values of our indicator  $I_t^{AC}$  for both the  $-4\%$  and  $-3\%$  crisis scenarios and for both the original signal and the smoothed (SM) signals. The red lines highlight the results for our indicator. (For interpretation of the references to colour in this figure legend, the reader is referred to the web version of this article.)

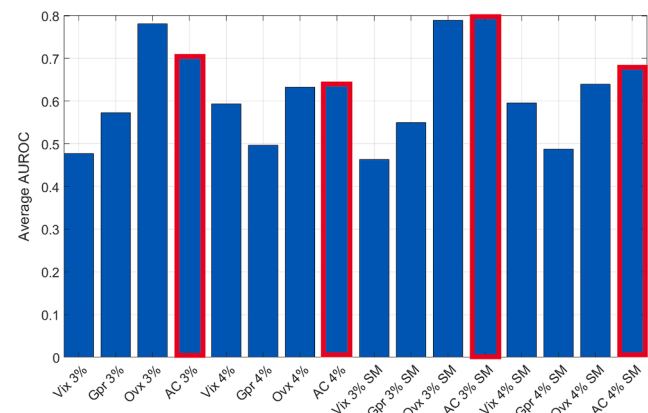


**Fig. 11.** Comparison of the AUROC values for the Asia/Pacific index. The blue bars represent the average AUROC values obtained with the Vix, the Gpr and the Ovx indices, along with the AUROC values of our indicator  $I_t^{AC}$  for both the  $-4\%$  and  $-3\%$  crisis scenarios and for both the original signal and the smoothed (SM) signals. The red lines highlight the results for our indicator. (For interpretation of the references to colour in this figure legend, the reader is referred to the web version of this article.)

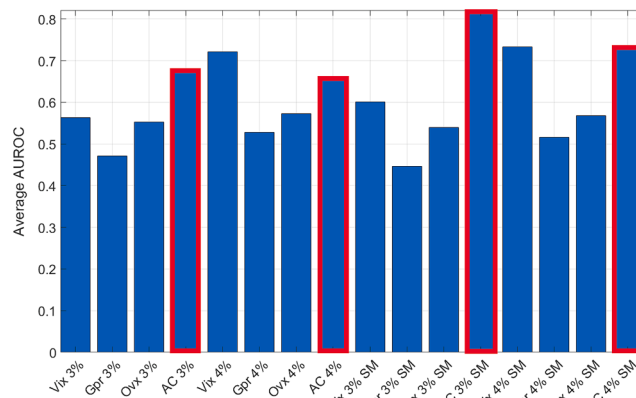


**Fig. 10.** Comparison of the AUROC values for the Europe index. The blue bars represent the average AUROC values obtained with the Vix, the Gpr and the Ovx indices, along with the AUROC values of our indicator  $I_t^{AC}$  for both the  $-4\%$  and  $-3\%$  crisis scenarios and for both the original signal and the smoothed (SM) signals. The red lines highlight the results for our indicator. (For interpretation of the references to colour in this figure legend, the reader is referred to the web version of this article.)

sentiments and it is usually considered as an indicator of risk, fear and financial stress. The Ovx represents the CBOE Crude Oil ETF Volatility Index and it measures the market's expectation of 30-day volatility of crude oil prices. It is computed by applying the Vix methodology to the United States Oil Fund options. Finally, we also compare our indicator against the Gpr indicator (see Caldara & Iacoviello, 2018), which is a monthly index of geopolitical risk counting the occurrence of words related to geopolitical tensions in leading international newspapers.

More specifically, we have computed the average values of the Vix, Ovx and Gpr using the same moving window  $w$  employed to calculate  $I_t^{AC}$ , and we have performed the same non-parametric analysis for both the  $-3\%$  and  $-4\%$  crisis scenarios, followed by averaging the AUROC values and comparing these values with the values produced by our indicator.

Figs. 9–11 reveal that, on average, our indicator outperforms the three alternative measures. In particular, while the Ovx shows a superior performance only in the case of  $-3\%$  crisis scenarios for the North America and Asia/Pacific markets and the Vix provides better

informative signals for the  $-4\%$  in the Europe 50 stock index, in all the other scenarios the LTM indicator  $I_t^{AC}$  has superior capabilities in anticipating crisis events. Moreover, notice that, on average, the worst performing indicator is the Gpr since it mainly considers events that primarily affect emerging markets which are not considered in our samples.

## 4. Discussion

### 4.1. Policy evaluation

The 2008–2009 global financial crisis has enhanced the debate on whether policy authorities should use measures to dampen the degree of financial overheating both through usual policy decisions and by signalling to the public their commitments about limiting financial imbalances. As a result, policymakers might more effectively maintain financial and price stability in the medium and long run. One of the main counter-arguments to implement “leaning against the wind” macro-prudential policies has been that the data do not provide a reliable signal to timely act, especially before the burst of financial markets. Thus, policymakers would need reliable indicators which identify hurtful financial cycles with sufficient lead time to take action (see Alessi & Detken, 2011; Bank for International Settlements, 2012; Spelta, Pecora, & Kaltwasser, 2019).

Moreover, the performance evaluation of early-warning indicators should be combined with a usefulness measure for the policymaker, which depends on the relative aversion against missed crises as opposed to false alarms in order to have a much restrictive criterion to assess the performance of the indicator.

To evaluate to what extent our proposed indicator would be useful for a policymaker, we follow the policy evaluation diagnostic proposed by Sarlin (2013). Basically, we formulate a loss function and usefulness measures that are functions of the unconditional probabilities of crisis events, the misclassification costs of both classes, and the policymakers' preferences between the two error types (see Section 2). In this way, we are able to capture some important stylized facts of crisis occurrences, such as the fact that financial turmoils are outlier events whose dynamics significantly differ from the ones observed during tranquil times, and the fact that crises are costly and rarely occur.

This signalling approach is used to forecast market crashes subject to policymakers' relative preferences with respect to missed crises and false alarms. In other words, we use a loss function to rank the tested

**Table 2**

Policy Analysis. Stock market: North America index. For different values of preferences ( $\mu$ ), we report the absolute usefulness ( $U_a$ ), the relative usefulness ( $U_r$ ) and the optimal threshold (Thresh.) for moving windows (w) of 10 days, 15 days and 20 days. Results refer to the –3% crisis scenario.

$\mu$	$U_a(\mu)$ w-10d	$U_r(\mu)$ w-10d	Thresh. w-10d	$U_a(\mu)$ w-15d	$U_r(\mu)$ w-15d	Thresh. w-15d	$U_a(\mu)$ w-20d	$U_r(\mu)$ w-20d	Thresh. w-20d
0.0000	–0.0000	NaN	0.4159	0.0000	NaN	0.4626	0.0000	NaN	0.3893
0.1000	0.0002	0.0100	0.3570	0.0004	0.0214	0.3162	0.0002	0.0138	0.3893
0.2000	0.0018	0.0523	0.0728	0.0017	0.0505	0.1314	0.0008	0.0231	0.2357
0.3000	0.0054	0.1049	0.0558	0.0047	0.0924	0.0828	0.0039	0.0760	0.0527
0.4000	0.0096	0.1411	0.0507	0.0093	0.1358	0.0697	0.0086	0.1257	0.0423
0.5000	0.0146	0.1714	0.0406	0.0148	0.1739	0.0607	0.0146	0.1710	0.0350
0.6000	0.0209	0.2044	0.0311	0.0213	0.2087	0.0528	0.0223	0.2173	0.0287
0.7000	0.0300	0.2522	0.0222	0.0299	0.2508	0.0349	0.0316	0.2648	0.0227
0.8000	0.0443	0.3257	0.0109	0.0440	0.3231	0.0148	0.0444	0.3252	0.0096
0.9000	0.0165	0.1984	0.0043	0.0178	0.2144	0.0051	0.0158	0.1907	0.0037
1.0000	0.0000	NaN	0.0010	0.0000	NaN	0.0010	0.0000	NaN	0.0010

**Table 3**

Policy Analysis. Stock market: Europe index. For different measures of preferences ( $\mu$ ), we report the absolute usefulness ( $U_a$ ), the relative usefulness ( $U_r$ ) and the optimal threshold (Thresh.) for moving windows (w) of 10 days, 15 days and 20 days. Results refer to the –3% crisis scenario.

$\mu$	$U_a(\mu)$ w-10d	$U_r(\mu)$ w-10d	Thresh. w-10d	$U_a(\mu)$ w-15d	$U_r(\mu)$ w-15d	Thresh. w-15d	$U_a(\mu)$ w-20d	$U_r(\mu)$ w-20d	Thresh. w-20d
0.0000	–0.0001	NaN	0.6932	–0.0002	NaN	0.7681	0.0000	NaN	0.3173
0.1000	0.0000	0.0011	0.6598	–0.0001	–0.0044	0.7681	0.0001	0.0054	0.3102
0.2000	0.0003	0.0072	0.4050	–0.0001	–0.0012	0.7368	0.0004	0.0082	0.2256
0.3000	0.0015	0.0202	0.2586	0.0002	0.0025	0.5155	0.0009	0.0126	0.1480
0.4000	0.0038	0.0390	0.1748	0.0024	0.0250	0.1135	0.0020	0.0206	0.0915
0.5000	0.0077	0.0635	0.1408	0.0061	0.0504	0.0973	0.0057	0.0471	0.0410
0.6000	0.0139	0.0964	0.0890	0.0121	0.0836	0.0675	0.0129	0.0888	0.0270
0.7000	0.0279	0.1653	0.0481	0.0282	0.1667	0.0271	0.0292	0.1726	0.0138
0.8000	0.0265	0.1748	0.0155	0.0260	0.1713	0.0113	0.0275	0.1811	0.0057
0.9000	0.0022	0.0296	0.0056	0.0020	0.0269	0.0036	0.0019	0.0255	0.0022
1.0000	0.0000	NaN	0.0010	0.0000	NaN	0.0010	0.0000	NaN	0.0010

**Table 4**

Policy Analysis. Stock market: Asia/Pacific index. For different measures of preferences ( $\mu$ ), we report the absolute usefulness ( $U_a$ ), the relative usefulness ( $U_r(\mu)$ ) and the optimal threshold (Thresh.) for moving windows (w) of 10 days, 15 days and 20 days. Results refer to the –3% crisis scenario.

$\mu$	$U_a(\mu)$ w-10d	$U_r(\mu)$ w-10d	Thresh. w-10d	$U_a(\mu)$ w-15d	$U_r(\mu)$ w-15d	Thresh. w-15d	$U_a(\mu)$ w-20d	$U_r(\mu)$ w-20d	Thresh. w-20d
0.0000	–0.0001	NaN	0.4825	–0.0001	NaN	0.5256	–0.0000	NaN	0.5490
0.1000	–0.0000	–0.0028	0.4344	0.0001	0.0042	0.5219	0.0001	0.0042	0.5407
0.2000	0.0002	0.0055	0.2966	0.0003	0.0094	0.4327	0.0002	0.0065	0.4451
0.3000	0.0008	0.0157	0.0983	0.0009	0.0181	0.2742	0.0008	0.0159	0.2222
0.4000	0.0023	0.0338	0.0508	0.0023	0.0326	0.1751	0.0023	0.0322	0.0961
0.5000	0.0058	0.0671	0.0306	0.0050	0.0573	0.1047	0.0047	0.0537	0.0636
0.6000	0.0130	0.1245	0.0193	0.0111	0.1065	0.0597	0.0095	0.0905	0.0372
0.7000	0.0253	0.2079	0.0142	0.0231	0.1893	0.0412	0.0216	0.1768	0.0238
0.8000	0.0426	0.3064	0.0114	0.0419	0.3006	0.0288	0.0423	0.3031	0.0165
0.9000	0.0068	0.0818	0.0028	0.0063	0.0768	0.0051	0.0066	0.0804	0.0035
1.0000	0.0000	NaN	0.0010	0.0000	NaN	0.0010	0.0000	NaN	0.0010

indicators given the relative preferences of policymakers with respect to missed crises and false alarms. More precisely, this approach provides useful information to decision makers in a timely manner by considering only the most significant crisis events.

Tables 2–4 report the results for the –3% crisis scenario, averaged along different moving windows. In line with the literature, our early-warning indicator outperforms the best-guess of a policymaker, meaning that the usefulness obtained by employing the indicator is greater than the usefulness achieved by never signaling any crisis, providing therefore an overall positive usefulness. As expected,  $I^{AC}$  provides a higher usefulness for policymakers more concerned with missing crises than with issuing false alarms. Finally, the tables show that, in general,

the optimal threshold (the threshold used to turn our continuous indicator into a binary prediction) decreases as long as the preference parameter  $\mu$  increases, implying more crisis signals in correspondence of larger  $\mu$ . This is a consequence of the fact that, when the perceived loss for missing crises is larger, then it is optimal to signal more. The relative usefulness is larger than 10% for  $\mu$  larger than 0.30 only in the case of the STOXX North America 600, while for the other two markets this happens for values of  $\mu$  larger than 0.60–0.70. This means that our indicator is able to correctly classify events according to the objective criterion defined by the usefulness measure, since it is more concerned about the rarer class (the crisis class) with respect to issuing false alarms.

All in all we believe that a preference parameter  $\mu$  around 0.5 may be



**Fig. 12.** Profit & Loss dynamic. Stock market: North America. The plot reports the cumulative Profit & Loss obtained by performing investment strategies based on the three indicators,  $I^{AC}$ ,  $I^{AC,STD}$  and  $I^{STD}$ , together with the cumulative performance of the benchmark index (proxy for STOXX North America 600). A short position is taken if the average value of the indicator (computed using the last 10 days) is higher than the value of the indicator computed in a tranquil market phase (January-June 2005), otherwise a long position is taken. In the first case the cumulative performance changes by  $\frac{P_t - P_{t+1}}{P_{t+1}}$ , in the second case by  $\frac{P_{t+1} - P_t}{P_t}$ . This helps in quantifying how the correct and timely forecast of boom and burst phases affects the overall cumulative performances. The results are obtained using the following parameters:  $w = 10$ ,  $x = 40\%$ .



**Fig. 13.** Profit & Loss dynamic. Stock market: Europe. The plot reports the cumulative Profit & Loss obtained by performing investment strategies based on the three indicators,  $I^{AC}$ ,  $I^{AC,STD}$  and  $I^{STD}$ , together with the cumulative performance of the benchmark index (proxy for STOXX Europe 50). A short position is taken if the average value of the indicator (computed using the last 10 days) is higher than the value of the indicator computed in a tranquil market phase (January-June 2005), otherwise a long position is taken. In the first case the cumulative performance changes by  $\frac{P_t - P_{t+1}}{P_{t+1}}$ , in the second case by  $\frac{P_{t+1} - P_t}{P_t}$ . The results are obtained using the following parameters:  $w = 10$ ,  $x = 40\%$ .

seen as a realistic value for the policymakers' loss functions. Indeed, if a financial crisis is not detected as such in a timely manner there always remains the possibility to smooth the crisis phase by means of an accommodating policy stance. On the contrary, a policymaker would certainly have to deal with a severe pressure when being found out to have issued a false alarm.

#### 4.2. Investment Strategies

To further motivate whether our proposed methodology is able to correctly identify changes in stock prices, a backtest based on a hypothetical investment strategy is implemented following the line of [Preis, Moat, and Stanley \(2013\)](#) and [Spelta \(2017\)](#). After having identified the first half of 2005 as a tranquil market phase, we use it as a reference period for implementing a possible investment strategy for a portfolio that employs the proposed early-warning indicator for stocks buy/sell decisions. This first step helps in quantifying the "natural" variability of the early-warning indicator during normal times. Notice that a positive performance (i.e., a profit) can be obtained with a trading strategy that correctly anticipates at least some future changes in the aggregate stock price indices, especially around large market movements.

Our illustrative strategy is based on the following procedure: if the

average value of the indicator over the past 10 days<sup>5</sup> is higher than the one computed on the first six months of the 2005, a short position is taken by selling the index and buying it back in the next trading day. In this case, the cumulative performance related to this index varies by  $\frac{P_t - P_{t+1}}{P_{t+1}}$  in the interval from  $t$  to  $t + 1$ . Otherwise, if the average value of the indicator is lower than the one in 2005, a long position is taken by buying the index and then selling it in the next trading day. The cumulative performance in this case changes by  $\frac{P_{t+1} - P_t}{P_t}$ . In this way, buying and selling actions have a symmetric impact on the cumulative performance of the portfolio strategy. For simplicity, we neglect transaction costs and management fees in the computation of the cumulative performance, even if they would impact the effective profitability and capacity of the strategy.

[Fig. 12](#) shows the cumulative Profit & Loss (P&L) obtained by investing in the STOXX North America 600 following the behavior of the indicators  $I^{AC}$ ,  $I^{STD}$  and  $I^{AC,STD}$  together with the cumulative performance obtained by simply following the market benchmark (in blue). From [Fig. 12](#) it is clear that the investment strategy based on our proposed indicator performs better than the benchmark index, and  $I^{AC}$  outperforms both  $I^{STD}$  and  $I^{AC,STD}$ . This result is due to the fact that, although in phases of business expansion the strategies based on the early-

<sup>5</sup> We have also performed robustness checks using different values of the averaging window (from 20 to 50 days). Results and investment implications remain qualitatively the same.



**Fig. 14.** Profit & Loss dynamic. Stock market: Asia/Pacific. The plot reports the cumulative Profit & Loss obtained by performing investment strategies based on the three indicators,  $I^{AC}$ ,  $I^{AC,STD}$  and  $I^STD$ , together with the cumulative performance of the benchmark index (proxy for STOXX Asia/Pacific 600). A short position is taken if the average value of the indicator (computed using the last 10 days) is higher than the value of the indicator computed in a tranquil market phase (January-June 2005), otherwise a long position is taken. In the first case the cumulative performance changes by  $\frac{P_{t+1}-P_t}{P_{t+1}}$ , in the second case by  $\frac{P_{t+1}-P_t}{P_t}$ . The results are obtained using the following parameters:  $w = 10$ ,  $x = 40\%$ .

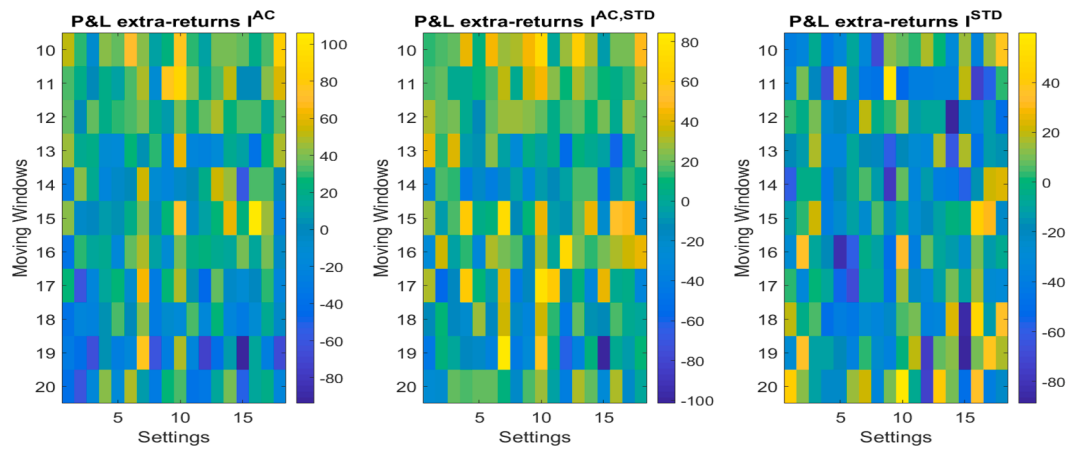


**Fig. 15.** Cumulative P&L obtained at the end of the time sample for different values of the parameters  $w$  and  $x$ . Stock market: North America. The plots show the difference between the cumulative returns obtained by following the early-warning indicators and the cumulative returns obtained following the market benchmark (proxy for STOXX North America 600). Each cell encompasses the end of sample cumulative P&L for pair values of the parameters  $w$  and  $x$ . The left panel shows the result for  $I^{AC}$ , the central panel regards the mixed signal  $I^{AC,STD}$  and the right panel refers to  $I^STD$ .

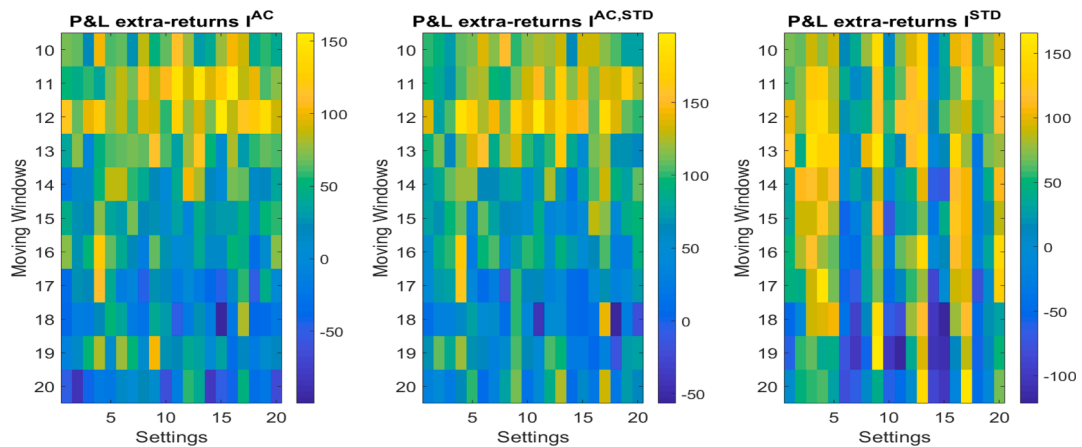


**Fig. 16.** Cumulative P&L obtained at the end of the time sample for different values of the parameters  $w$  and  $x$ . Stock market: Europe. The plots show the difference between the cumulative returns obtained by following the early warning indicators and the cumulative returns obtained following the market benchmark (proxy for STOXX Europe 50). Each cell encompasses the end of sample cumulative P&L for pair values of the parameters  $w$  and  $x$ . The left panel shows the result for  $I^{AC}$ , the central panel regards the mixed signal  $I^{AC,STD}$  and the right panel refers to  $I^STD$ .

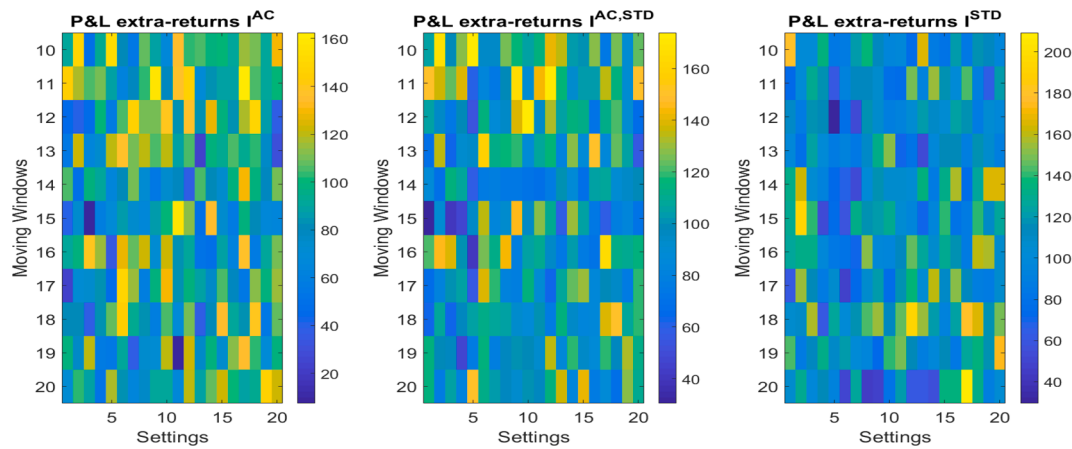


**Fig. 17.** Cumulative P&L obtained at the end of the time sample for different values of the parameters  $w$  and  $x$ . Stock market: Asia/Pacific. The plots show the difference between the cumulative returns obtained by following the early-warning indicators and the cumulative returns obtained following the market benchmark (proxy for STOXX Asia/Pacific 600). Each cell encompasses the end of sample cumulative P&L for pair values of the parameters  $w$  and  $x$ . The left panel shows the result for  $I^{AC}$ , the central panel regards the mixed signal  $I^{AC,STD}$  and the right panel refers to  $I^{STD}$ .

**Table 5**

Percentage annual performance for different moving windows. Stock market: North America. The table represents the annual performance of the proposed investment strategy for different values of the moving window parameter (indicated with  $w$ ) that ranges from 10 days to 20 days, along with the performance of the benchmark index,  $Ben$ , (proxy for STOXX North America 600). The annual performances are averaged across different values of the parameter  $x$ , that varies from 100% to 40%, defining the percentage of stocks used for the clustering procedure.

$w$	2005	2006	2007	2008	2009	2010	2011	2012	2013	2014	2015	2016	2017	2018
10	5.35	13.81	10.33	52.59	-14.77	8.60	19.98	-3.38	17.71	27.17	4.85	-4.29	4.52	3.55
11	-0.09	13.96	8.80	51.79	-14.29	16.84	11.52	-0.63	23.46	25.51	3.27	-7.39	4.61	3.55
12	-1.99	11.40	11.79	52.37	-15.13	15.79	14.42	-1.86	26.37	20.79	2.34	-6.92	4.10	3.55
13	3.98	14.66	6.24	52.37	-16.44	14.90	-1.07	-1.65	25.30	17.09	1.40	-6.23	4.63	3.55
14	7.29	13.83	11.72	52.37	-15.92	13.00	5.27	-6.21	24.21	12.51	-0.35	-8.27	4.54	3.55
15	10.48	15.95	11.45	52.38	-17.21	9.73	1.81	-2.45	28.01	19.34	4.02	-6.47	3.19	3.55
16	8.87	12.15	9.36	52.37	-15.54	13.89	2.50	-2.94	17.86	20.39	3.12	-1.56	1.54	3.55
17	7.89	10.69	10.28	52.37	-14.72	12.55	-3.87	0.63	17.82	16.81	2.49	-3.44	1.07	3.04
18	9.52	12.23	11.94	51.87	-15.21	9.59	-6.22	-2.22	17.55	18.87	-0.89	-3.30	-1.02	3.55
19	5.60	10.67	12.46	52.37	-16.58	5.87	-2.54	-2.35	14.78	15.57	-6.26	-7.63	-0.27	3.47
20	9.27	11.42	10.42	52.37	-16.89	12.06	-4.04	-4.25	12.27	14.90	6.87	0.74	-2.83	3.55
Ben.	8.85	2.26	-3.02	-34.78	23.26	20.80	3.55	11.25	20.68	24.12	10.43	13.39	4.95	3.55

**Table 6**

Percentage annual performance for different moving windows. Stock market: Europe. The table represents the annual performance of the proposed investment strategy for different values of the moving window parameter (indicated with  $w$ ) that ranges from 10 days to 20 days, along with the performance of the benchmark index,  $Ben$ , (proxy for STOXX Europe 50). The annual performances are averaged across different values of the parameter  $x$ , that varies from 100% to 40%, defining the percentage of stocks used for the clustering procedure.

$w$	2005	2006	2007	2008	2009	2010	2011	2012	2013	2014	2015	2016	2017	2018
10	10.18	-7.49	5.80	64.17	1.43	14.34	31.31	0.49	5.01	-0.78	-0.97	5.67	3.55	3.90
11	13.14	-1.51	6.34	65.95	-0.47	26.87	31.34	-1.74	9.46	-2.73	-0.28	-0.37	5.96	4.28
12	2.87	-0.52	12.45	64.58	2.65	22.54	34.41	-2.95	11.23	5.27	-1.18	5.36	7.00	4.48
13	10.70	-9.56	10.47	58.22	-8.44	5.87	33.33	0.49	13.28	4.95	1.87	-5.76	2.70	4.53
14	11.54	-16.23	18.61	61.38	-13.85	3.18	30.15	-1.29	7.51	-2.07	-2.88	0.06	5.03	4.31
15	14.43	-10.57	19.14	58.77	-6.27	-18.66	34.76	-3.21	8.56	-0.39	-7.69	0.98	7.19	4.57
16	19.38	-3.98	12.31	59.07	-14.47	-3.08	35.19	-2.05	4.58	-7.08	-6.33	3.06	6.68	4.64
17	14.52	-7.84	13.92	58.53	-12.77	-15.35	27.27	-1.22	1.04	-4.71	-3.36	5.08	6.70	4.84
18	11.02	-8.45	6.01	56.09	-5.28	-10.02	30.61	1.04	-5.07	-8.74	-6.76	-0.39	6.34	2.37
19	13.58	-7.14	18.33	59.06	-3.07	-7.65	30.44	-0.85	-8.90	-3.20	-2.71	3.58	4.94	4.44
20	13.24	-6.63	7.58	55.90	-3.84	-23.75	29.53	-0.05	-0.49	0.95	-21.69	-3.20	3.93	4.53
Ben.	19.91	15.16	7.83	-50.95	23.15	-3.16	-14.44	15.09	17.79	2.66	6.51	3.10	6.82	4.53

**Table 7**

Percentage annual performance for different moving windows. Stock market: Asia/Pacific. The table represents the annual performance of the proposed investment strategy for different values of the moving window parameter (indicated with  $w$ ) that ranges from 10 days to 20 days, along with the performance of the benchmark index, *Ben.*, (proxy for STOXX Asia/Pacific 600). The annual performances are averaged across different values of the parameter  $x$ , that varies from 100% to 40%, defining the percentage of stocks used for the clustering procedure.

$w$	2005	2006	2007	2008	2009	2010	2011	2012	2013	2014	2015	2016	2017	2018
10	17.81	-5.26	7.91	42.80	9.11	10.94	5.91	12.18	-5.23	20.17	44.66	3.04	7.34	3.07
11	18.94	-4.62	8.96	47.02	11.17	11.62	4.56	10.26	-4.29	22.43	41.76	0.87	7.83	3.07
12	18.38	-5.93	9.41	44.50	10.67	14.48	3.00	13.11	-6.08	20.52	37.72	-1.54	7.44	3.07
13	18.97	-6.66	6.39	40.97	5.85	12.58	6.17	10.93	0.05	22.46	37.17	0.27	7.48	3.07
14	17.06	-5.60	6.90	45.60	8.72	15.76	1.53	10.32	-0.63	20.25	37.40	-9.57	7.42	3.07
15	14.79	-8.07	6.39	44.12	10.32	12.93	5.48	12.80	-3.76	18.99	32.03	-5.35	7.89	3.07
16	17.00	-9.91	6.12	41.06	21.32	14.71	2.83	12.65	4.15	16.53	35.92	-6.76	7.55	3.07
17	18.31	-10.80	4.49	41.24	15.25	11.80	6.86	10.73	9.94	18.57	33.63	-9.11	7.54	3.07
18	16.14	-5.51	4.99	41.06	16.70	14.02	1.24	12.11	10.15	16.02	31.99	-7.10	7.65	3.07
19	15.65	-12.94	6.71	47.67	5.06	16.60	9.60	13.28	10.64	17.35	29.74	-11.66	7.39	3.07
20	11.81	-8.46	6.34	44.48	7.52	12.22	16.14	12.78	14.98	16.37	29.84	-6.14	7.33	3.07
Ben.	26.17	-0.16	-4.54	-35.46	17.70	20.10	-11.65	9.96	10.81	9.19	14.35	6.57	7.33	3.07

warning indicators perform very similar to the benchmark, during crisis periods the investment strategy based on our proposed indicator consistently overperforms the market index. Similarly, Fig. 13 shows the cumulative performance obtained by investing in the STOXX Europe 50 aggregate index. Again, the investment strategies based on the early-warning indicators perform better than the benchmark but in this case the performances produced by  $I^{STD}$  are the highest. Finally, Fig. 14 presents the cumulative performance for the STOXX Asia/Pacific 600 aggregate index. In this case the P&L obtained by employing  $I^C$  is the highest at the end of the sample period, together with the P&L related to the mixed signal  $I^{AC,STD}$ , while the indicator proposed by Chen et al. (2012) is the worst performer.

#### 4.2.1. Sensitivity analysis on investment strategies

All the figures reported above refer to the cumulative P&L for a specific value of  $w$  and  $x$ , but results may vary as long as these parameters change. Since the parameter space involves different values of  $w$  and  $x$ , a sensitivity analysis is needed for investigating the robustness of the method against different parameter settings. The sensitivity analysis is performed by letting  $w$  and  $x$  range in a grid of values along the simulations in order to study how these changes influence the overall final performance. Figs. 15–17 present, in each subplot, the sensitivity of the methodology to parameters' variation by indicating the cumulative P&L obtained at the end of the sample period.

Results indicate that the cumulative P&L are positive and higher for small values of the parameter  $w$  representing the moving window employed for computing the PCC. These results reinforce the idea that, although the length of the moving window determines a trade-off between the statistically significance of the signal and its ability to timely intercept changes in the system's behaviour, the adoption of a short moving window generates better P&Ls of the early-warning indicators. Moreover, for most of the parameter configurations, the portfolio strategy based on  $I^C$  outperforms the strategies based on either  $I^{AC,STD}$  or  $I^{AC,STD}$ . Additionally, only for the STOXX Asia/Pacific 600 aggregate index, results indicate that the cumulative P&Ls are positive for all parameter configurations, meaning that the benchmark is constantly outperformed by the strategies that employ these early-warning indicators.

Finally, Tables 5–7 show the annual performances of the hypothetical investment strategies, based on the indicator  $I^C$ , for the three financial markets along with the P&L obtained by following the market

benchmark. Results are represented for different values of the moving window parameter and averaged across different values of the parameter  $x$  defining the percentage of stocks used for the clustering procedure. In particular, Table 5 regards the STOXX North America 600 index, Table 6 refers to the STOXX Europe 50 index and Table 7 to the STOXX Asia/Pacific 600 index. From the tables, three interesting facts emerge. First, this illustrative investment strategy outperforms the benchmark during the years 2007–2008 and 2011, i.e., in the proximity of severe financial crises; secondly, the indicator takes time to intercept the end of the crisis, and thus the investment strategy performs poorly with respect to the benchmark in the years 2009 and 2012 (especially in Europe and US); thirdly, once the rebound due to the crisis has been absorbed, the proposed strategy performs in line with the benchmark during expansionary market phases.

## 5. Conclusions

Essential to the notion of financial complexity is the analysis of the interconnected patterns of stocks' returns. During market crises, investors generally allocate portfolios to safer assets (see e.g., Bethke, Gehde-Trapp, & Kempf, 2017; Kacperczyk & Schnabl, 2010; Rösch & Kaserer, 2013 among others), thus ensuring a flight to quality selection of stocks that could impact on the overall similarity of portfolio performances and, possibly, to the effective extent of diversification. The topological investigation of the financial market as a complex networked system is thus useful to recognize such patterns.

In this paper we have focused on the parsimonious detection of discontinuities in the dynamic laws that rule the evolution of a financial system. In the spirit of Orsenigo et al. (2001), Pammolli and Riccaboni (2002), Riccaboni and Pammolli (2003), and Pyka and Scharnhorst (2009), we have introduced a network-based synthetic indicator that reflects the varying intensity of market comovements and can be used as a marker for upcoming instabilities in financial markets. We have shown that the emergence of a sub-graph of stocks - the Leading Temporal Module - characterized by both high cohesiveness among its members and high autocovariance, signals an increased fragility of the actual rules governing the dynamics of the underlying market. This topological approach does not postulate any functional form for the laws of motion of the underlying system, but it exploits the qualitative and quantitative modifications of the correlation matrix to infer the presence of a metastable state, which can precede a market phase transition.

Namely, we have proposed a methodology to detect early-warning signals of phase transitions in financial markets by translating into mathematical terms the behavioral factors that have been found at the ground of many different financial crises. For developing our early-warning indicator, we have interpreted the increased autocovariance of stocks' returns as a signal of the presence of positive feedbacks, while the increased correlation among stocks' returns is referred to the presence of herding behaviors.

From a policy design perspective, our analysis has shown that the identification of the LTM as an indicator for an incoming market distress may constitute an important element for designing effective macro-prudential policies. A constant monitoring of stocks' returns that present high correlated patterns turns out to be crucial to check whether a repositioning of the investors' behavior is likely to generate an increasing fragility of the whole underlying financial system.

Finally, we have also implemented an illustrative investment strat-

egy that builds on the LTM to show how this approach can be effectively exploited to detect market phases by directly analyzing the evolution of the topological properties of the LTM sub-graph in different points in time. The proposed approach is model-free and its superior performance, compared with reasonable benchmark strategies, supports its usefulness for the timely activation and exploitation of investment strategies.

#### Declaration of Competing Interest

None.

#### Acknowledgements

The authors wish to thank two anonymous referees for their valuable comments and suggestions. The usual caveats apply.

#### Appendix A. Notations

The following table summarizes the notation employed throughout the paper (see Table A.8).

**Table A.8**  
List of abbreviations and symbols.

	Symbols	Definition	Symbols	Definition
LTM indicator	$P$	Stocks' Price	$G$	Graph
	$z$	Stocks' Return	$N$	Number of Stocks
	$t$	Time Stamp	$E$	Edges
	$N^{LTM}$	Stocks in LTM	$PCC$	Pearson Correlation Coefficient
	$N^o$	Stocks outside TLM	$STD$	Standard Deviation
	$AC$	Autocovariance	$I$	Early-Warning Indicator
	$\langle \cdot \rangle$	Average	$ \cdot $	Absolute Value
	$H$	$H$ -th Cluster members	$C$	Max number of Clusters
	$T$	Reporting Days	$Sil$	Sihouette
	$w$	Moving window length	$N_1$	Stocks with the highest AC
	$x$	Percentage of stocks with the highest AC retained	$numClust$	Number of clusters
	$z_1$	Returns of the stocks with the highest AC		
Non-parametric Analysis	$L$	Crises Indicator	$\tau$	Threshold for non-parametric Analysis
	$p$	Normalized Indicator	$B$	Binary Crisis indicator
	FP	False Positive	TP	True Positive
	FN	False Negative	TN	True Negative
	FPR	False Positive rate	TPR	True Positive rate
	P	Precision	R	Recall
	ROC	Receiver Operating Characteristics	PR	Precision-Recall Curve
	AUROC	Area under the ROC	AUPR	Area under PR Curve
Policy Analysis	$P_1$	Crises Frequency	$P_2$	Tranquil days Frequency
	$Lo$	Loss Function	$\mu$	Policy Maker Preferences
	$U_a$	Absolute Usefulness	$U_r$	Relative Usefulness

## Appendix B. Algorithm

### Algorithm 1. Pseudo-code

```

input :  $N \times T$  matrix of stock prices  $P$ , a moving window  $w$ , a cut parameter  $x$  for retaining stock with highest autocovariance, the maximum number of clusters  $C$ 
output:  $1 \times T$  vector denoting the early-warning signal  $I^{AC}$ 
//Compute returns
 $Z = \Delta(\log(P))$ 
//Find the number of stocks: stock ID
 $N = \text{size}(Z, 1)$ 
for  $k = 1$  to  $T - w - 1$  do
    //Extract returns from day  $k$  up to day  $k+w$ 
     $z = Z(:, k : k + w)$ 
    //Compute autocovariance
     $atc = \text{autocov}(z)$ 
    //Sort autocovariance in descending order
     $[S\ atc, pos] = \text{sort}(atc)$ 
    //Sort returns according to autocovariance
     $z_s = z(pos, :)$ 
    //Sort stocks ID according to autocovariance
     $N_s = N(pos)$ 
    //Take returns of stocks with high autocovariance
     $z_1 = z_s(1 : x, :)$ 
    //Take the ID of the stocks with high autocovariance
     $N_1 = N_s(1 : x)$ 
    for  $i = 2$  to  $C$  do
        //Partition of the returns with high autocovariance into  $C$  clusters
         $z_i = \text{cluster}(z_1, i)$ 
        //Compute the Silhouette value of the partition
         $sil_i = \text{Silhouette}(z_{clust})$ 
    //Find the maximum value of the Silhouette and the optimal number of cluster
     $[h, numClust] = \text{maxSil}(sil)$ 
    for  $c = 1$  to  $numClust$  do
        //Find cluster members
         $H = \text{members}(N_1, c)$ 
        //Compute the within absolute average correlation
         $<|PCC^H|> = \text{mean}(\text{corr}(z_1(H, :)))$ 
        //Compute the absolute average autocovariance of the cluster
         $<|AC^H|> = \text{mean}(\text{autocov}(z_1(H, :)))$ 
        //Compute the between absolute average correlation
         $<|PCC^{N_1 \setminus H}|> = \text{mean}(\text{corr}(z_1(N_1 \setminus H)))$ 
        //Compute cluster indicator
         $I^{AC,H} = \frac{|AC^H| < |PCC^H|}{|PCC^{N_1 \setminus H}|}$ 
    //Compute Early-Warning Indicator
     $t = k + w$ 
     $I_t^{AC} = \max(I^{AC,H})$ 

```

## Appendix C. Robustness analysis

In order to show the robustness of the main findings to changes in the values of the parameter  $x$ , representing the percentage of stocks selected for the clustering procedure, we report in Tables C.9–C.11, the average AUROC values obtained by letting the parameter  $x$  to vary from 100% to 40%. Table C.9 clearly shows that, for the STOXX North America 600 index, our proposed indicator  $I_t^{AC}$  produces, on average, the highest AUROC values, outperforming the other two early-warning indicators. The mixed signal comes second and  $I_t^{STD}$  follows. Notice that, in all the settings, our method generates quite high AUROC values, around 75–80%, meaning that it contains useful information to forecast crisis events. This occurrence can be traced back to the fact that the autocovariance is more able to capture positive feedbacks generated on the market during pre-crisis phases. Only in the –3% crisis scenario the smoothed signals perform similarly. For the STOXX Europe 50 index (see Table C.10),  $I_t^{AC}$  and the mixed signal  $I_t^{AC,STD}$  produce similar results and, depending on  $x$  and on the type of scenario, the former can be slightly better than the latter but both overcome the indicator  $I_t^{STD}$  proposed in Chen et al. (2012). Finally, for the STOXX Asia/Pacific 600 index (see Table C.11), we observe that the mixed signal  $I_t^{AC,STD}$  together with  $I_t^{AC}$  produces, on average, the best results, but in few cases the  $I_t^{STD}$  indicator outperforms the others.

Proceeding as with the AUROC values, we show the results of the robustness check regarding the AUPR values. Tables C.12–C.14 highlight how findings modify to changes in the value of the parameter  $x$ . Generally speaking, in the case of AUPR, the mixed signal  $I_t^{AC,STD}$  produces the best performance in all of the three datasets, while our indicator  $I_t^{AC}$  follows with few exceptions, as in the case of the STOXX Europe 50 index and the –4% crisis scenario where the  $I_t^{STD}$  comes second.

**Table C.9**

Average AUROC values for different settings of the parameter  $x$ , defining the percentage of stocks with the highest autocovariance (standard deviation) used for the clustering procedure. Stock market: North America. The table represents the average AUROC values obtained by varying the parameter  $x$  used to select the financial instruments (referring to STOXX North America 600) with the highest autocovariance in the case of  $I_t^{AC}$ , or standard deviation for  $I_t^{STD}$ . The parameter  $x$  varies from 100% to 40%. For the mixed case, we select the intersection of the stocks extracted by the previous settings (autocovariance and standard deviation). The first three columns refer to the –4% crisis scenario for  $I_t^{AC,STD}$ ,  $I_t^{AC}$  and  $I_t^{STD}$ , respectively. Columns four to six refer to the –4% crisis scenario and to the smoothed (SM) indicators. Columns seven to nine refer to the –3% scenario and the last three columns encompass the AUROC values of the smoothed (SM) indicators for the –3% crisis scenario.

4% Std + Ac	4% Ac	4% Std	4%-SM Std + Ac	4%-SM Ac	4%-SM Std	3% Std + Ac	3% Ac	3% Std	3%-SM Std + Ac	3%-SM Ac	3%-SM Std
0.7480	0.7752	0.7045	0.7642	0.8002	0.7317	0.7324	0.7709	0.7395	0.7921	0.8375	0.7546
0.7580	0.7723	0.7027	0.7628	0.7961	0.7296	0.7427	0.7656	0.7392	0.7912	0.8303	0.7569
0.7488	0.7642	0.7033	0.7629	0.7984	0.7376	0.7377	0.7544	0.7330	0.7882	0.8327	0.7493
0.7637	0.7737	0.7031	0.7610	0.8002	0.7303	0.7498	0.7694	0.7331	0.7926	0.8427	0.7493
0.7542	0.7638	0.7041	0.7556	0.7967	0.7367	0.7470	0.7554	0.7364	0.7886	0.8292	0.7519
0.7552	0.7583	0.7008	0.7502	0.7899	0.7304	0.7422	0.7480	0.7286	0.7805	0.8179	0.7425
0.7683	0.7770	0.7101	0.7732	0.8041	0.7389	0.7565	0.7721	0.7338	0.7953	0.8517	0.7524
0.7546	0.7725	0.7006	0.7538	0.7947	0.7326	0.7334	0.7631	0.7278	0.7842	0.8292	0.7413
0.7626	0.7682	0.7016	0.7504	0.7936	0.7306	0.7492	0.7572	0.7319	0.7827	0.8213	0.7456
0.7489	0.7523	0.6957	0.7459	0.7826	0.7185	0.7386	0.7417	0.7225	0.7742	0.8161	0.7345
0.7550	0.7745	0.7052	0.7684	0.8021	0.7347	0.7382	0.7670	0.7300	0.7932	0.8439	0.7494
0.7586	0.7706	0.7034	0.7520	0.7946	0.7346	0.7444	0.7597	0.7316	0.7824	0.8229	0.7431
0.7464	0.7565	0.6983	0.7471	0.7894	0.7277	0.7392	0.7438	0.7274	0.7813	0.8158	0.7415
0.7446	0.7535	0.6970	0.7487	0.7864	0.7262	0.7329	0.7406	0.7237	0.7769	0.8118	0.7373
0.7524	0.7760	0.7044	0.7538	0.8018	0.7403	0.7304	0.7626	0.7258	0.7857	0.8356	0.7414
0.7504	0.7758	0.7065	0.7717	0.8034	0.7319	0.7348	0.7715	0.7431	0.7946	0.8480	0.7608
0.7499	0.7748	0.7041	0.7693	0.8000	0.7294	0.7356	0.7739	0.7447	0.7976	0.8414	0.7621
0.7564	0.7715	0.7015	0.7705	0.7961	0.7289	0.7466	0.7678	0.7413	0.7946	0.8304	0.7571

**Table C.10**

Average AUROC values for different settings of the parameter  $x$ , defining the percentage of stocks with the highest autocovariance (standard deviation) used for the clustering procedure. Stock market: Europe. The table represents the average AUROC values obtained by varying the parameter  $x$  used to select the financial instruments (referring to STOXX Europe 50) with the highest autocovariance in the case of  $I_t^{AC}$ , or standard deviation for  $I_t^{STD}$ . The parameter  $x$  varies from 100% to 40%. For the mixed case, we select the intersection of the stocks extracted by the previous settings (autocovariance and standard deviation). The first three columns refer to the –4% crisis scenario for  $I_t^{AC,STD}$ ,  $I_t^{AC}$  and  $I_t^{STD}$ , respectively. Columns four to six refer to the –4% crisis scenario and to the smoothed (SM) indicators. Columns seven to nine refer to the –3% scenario and the last three columns encompass the AUROC values of the smoothed (SM) indicators for the –3% crisis scenario.

4% Std + Ac	4% Ac	4% Std	4%-SM Std + Ac	4%-SM Ac	4%-SM Std	3% Std + Ac	3% Ac	3% Std	3%-SM Std + Ac	3%-SM Ac	3%-SM Std
0.6631	0.6776	0.6514	0.7386	0.7527	0.7232	0.6784	0.6868	0.6181	0.8467	0.8300	0.7199
0.6630	0.6717	0.6419	0.7376	0.7512	0.7179	0.6820	0.6831	0.6121	0.8448	0.8227	0.7034
0.6631	0.6566	0.6262	0.7285	0.7319	0.6837	0.6875	0.6738	0.5974	0.8447	0.8180	0.6678
0.6935	0.6878	0.6450	0.7183	0.7444	0.6836	0.7153	0.6926	0.6365	0.8546	0.8375	0.7658
0.6580	0.6727	0.6515	0.7302	0.7463	0.7274	0.6701	0.6816	0.6116	0.8445	0.8277	0.7213
0.6605	0.6522	0.6239	0.7242	0.7330	0.6846	0.6862	0.6723	0.5906	0.8425	0.8149	0.6538
0.6582	0.6382	0.6093	0.7148	0.7139	0.6579	0.6799	0.6543	0.5641	0.8387	0.8016	0.6086
0.6648	0.6809	0.6487	0.7164	0.7432	0.6991	0.6847	0.6891	0.6263	0.8475	0.8328	0.7492
0.6530	0.6569	0.6445	0.7234	0.7368	0.7168	0.6738	0.6777	0.6007	0.8424	0.8249	0.6945
0.6523	0.6431	0.6272	0.7157	0.7240	0.6860	0.6824	0.6711	0.5915	0.8411	0.8148	0.6538
0.6512	0.6242	0.5996	0.7030	0.6899	0.6354	0.6756	0.6453	0.5518	0.8362	0.7887	0.5855
0.6566	0.6626	0.6466	0.7089	0.7267	0.6968	0.6805	0.6830	0.6183	0.8455	0.8310	0.7222
0.6526	0.6453	0.6266	0.7165	0.7235	0.6936	0.6751	0.6709	0.5875	0.8359	0.8109	0.6564
0.6526	0.6356	0.6137	0.7082	0.7058	0.6534	0.6797	0.6588	0.5722	0.8373	0.7997	0.6128
0.6514	0.6280	0.6037	0.7056	0.6973	0.6380	0.6773	0.6490	0.5557	0.8379	0.7924	0.5897
0.6545	0.6626	0.6434	0.7126	0.7273	0.6973	0.6773	0.6823	0.6071	0.8379	0.8155	0.6896
0.6973	0.6900	0.6491	0.7306	0.7493	0.6999	0.7167	0.6966	0.6289	0.8596	0.8467	0.7703
0.6681	0.6852	0.6525	0.7455	0.7560	0.7288	0.6823	0.6951	0.6270	0.8540	0.8419	0.7461
0.6660	0.6827	0.6502	0.7444	0.7563	0.7286	0.6817	0.6940	0.6196	0.8511	0.8367	0.7261
0.6668	0.6736	0.6386	0.7418	0.7517	0.7155	0.6886	0.6869	0.6129	0.8495	0.8294	0.7074

**Table C.11**

Average AUROC values for different settings of the parameter  $x$ , defining the percentage of stocks with the highest autocovariance (standard deviation) used for the clustering procedure. Stock market: Asia/Pacific. The table represents the average AUROC values obtained by varying the parameter  $x$  used to select the financial instruments (referring to STOXX Asia/Pacific 600) with the highest autocovariance in the case of  $I_t^{AC}$ , or standard deviation for  $I_t^{STD}$ . The parameter  $x$  varies from 100% to 40%. For the mixed case, we select the intersection of the stocks extracted by the previous settings (autocovariance and standard deviation). The first three columns refer to the –4% crisis scenario for  $I_t^{AC,STD}$ ,  $I_t^{AC}$  and  $I_t^{STD}$ , respectively. Columns four to six refer to the –4% crisis scenario and to the smoothed (SM) indicators. Columns seven to nine refer to the –3% scenario and the last three columns encompass the AUROC values of the smoothed (SM) indicators for the –3% crisis scenario.

4% Std + Ac	4% Ac	4% Std	4%-SM Std + Ac	4%-SM Ac	4%-SM Std	3% Std + Ac	3% Ac	3% Std	3%-SM Std + Ac	3%-SM Ac	3%-SM Std
0.6490	0.6462	0.6248	0.6807	0.6832	0.6696	0.7126	0.7060	0.6923	0.8087	0.8037	0.8013
0.6434	0.6386	0.6222	0.6772	0.6787	0.6658	0.7125	0.7059	0.6958	0.8063	0.8018	0.7934
0.6399	0.6370	0.6119	0.6772	0.6803	0.6574	0.7126	0.7107	0.6920	0.8073	0.8051	0.7899
0.6576	0.6515	0.6412	0.6959	0.6940	0.7014	0.7139	0.7092	0.6992	0.8064	0.8004	0.8056
0.6409	0.6450	0.6282	0.6865	0.6876	0.6799	0.7016	0.7078	0.6907	0.8043	0.7973	0.7969
0.6368	0.6397	0.6146	0.6784	0.6808	0.6593	0.7023	0.7094	0.6901	0.8066	0.8040	0.7904
0.6348	0.6359	0.6073	0.6766	0.6801	0.6596	0.7021	0.7083	0.6859	0.8127	0.8088	0.7969
0.6571	0.6527	0.6387	0.6968	0.6977	0.6992	0.7166	0.7124	0.6988	0.8042	0.7980	0.8001
0.6397	0.6435	0.6212	0.6804	0.6824	0.6746	0.7017	0.7069	0.6920	0.8020	0.7969	0.7950
0.6381	0.6423	0.6154	0.6762	0.6786	0.6611	0.7039	0.7036	0.6879	0.7988	0.7957	0.7892
0.6430	0.6393	0.6093	0.6787	0.6803	0.6591	0.7057	0.7011	0.6775	0.8029	0.7992	0.7854
0.6524	0.6485	0.6359	0.6902	0.6912	0.6957	0.7166	0.7107	0.7034	0.8020	0.7954	0.7986
0.6409	0.6471	0.6184	0.6776	0.6808	0.6642	0.6973	0.7051	0.6868	0.7982	0.7944	0.7773
0.6437	0.6410	0.6101	0.6792	0.6812	0.6560	0.7109	0.7093	0.6881	0.8097	0.8058	0.7904
0.6294	0.6342	0.6047	0.6784	0.6816	0.6622	0.7010	0.7068	0.6833	0.8072	0.8068	0.7912
0.6537	0.6506	0.6299	0.6879	0.6904	0.6843	0.7179	0.7133	0.6973	0.7998	0.7948	0.7924
0.6479	0.6485	0.6345	0.6910	0.6920	0.6891	0.7157	0.7141	0.7004	0.8121	0.8050	0.8150
0.6483	0.6481	0.6297	0.6853	0.6870	0.6775	0.7121	0.7102	0.6937	0.8108	0.8056	0.8066
0.6468	0.6425	0.6209	0.6785	0.6829	0.6658	0.7149	0.7094	0.6926	0.8086	0.8040	0.7977
0.6372	0.6407	0.6207	0.6780	0.6816	0.6642	0.7039	0.7092	0.6971	0.8066	0.8013	0.8000

**Table C.12**

Average AUPR values for different settings of the parameter  $x$ , defining the percentage of stocks with the highest autocovariance (or standard deviation) used for the clustering procedure. Stock market: North America. The table represents the average AUPR values obtained by varying the parameter  $x$  used to select the financial instruments (referring to STOXX North America 600) with the highest autocovariance in the case of  $I_t^{AC}$ , or standard deviation for  $I_t^{STD}$ . The parameter  $x$  varies from 100% to 40%. For the mixed case, we select the intersection of the stocks extracted by the previous settings (autocovariance and standard deviation). The first three columns refer to the –4% crisis scenario for  $I_t^{AC,STD}$ ,  $I_t^{AC}$  and  $I_t^{STD}$ , respectively. Columns four to six refer to the –4% crisis scenario and to the smoothed (SM) indicators. Columns seven to nine refer to the –3% scenario and the last three columns encompass the AUPR values of the smoothed (SM) indicators for the –3% crisis scenario.

4% Std + Ac	4% Ac	4% Std	4%-SM Std + Ac	4%-SM Ac	4%-SM Std	3% Std + Ac	3% Ac	3% Std	3%-SM Std + Ac	3%-SM Ac	3%-SM Std
0.0508	0.0458	0.0289	0.0692	0.0688	0.0531	0.5028	0.4916	0.3567	0.5149	0.6422	0.3698
0.0509	0.0438	0.0290	0.0688	0.0678	0.0528	0.5044	0.4818	0.3596	0.5190	0.6388	0.3811
0.0512	0.0433	0.0297	0.0693	0.0673	0.0543	0.5017	0.4736	0.3510	0.5217	0.6372	0.3727
0.0501	0.0447	0.0291	0.0696	0.0690	0.0522	0.4988	0.4875	0.3498	0.5162	0.6421	0.3632
0.0515	0.0427	0.0304	0.0701	0.0677	0.0581	0.5087	0.4788	0.3556	0.5299	0.6358	0.3821
0.0490	0.0403	0.0281	0.0691	0.0656	0.0561	0.4987	0.4657	0.3500	0.5294	0.6265	0.3868
0.0512	0.0485	0.0264	0.0704	0.0700	0.0528	0.5088	0.5009	0.3500	0.5324	0.6508	0.3715
0.0503	0.0444	0.0299	0.0695	0.0682	0.0563	0.4936	0.4765	0.3479	0.5139	0.6342	0.3652
0.0509	0.0422	0.0299	0.0705	0.0677	0.0578	0.4975	0.4709	0.3463	0.5237	0.6283	0.3712
0.0485	0.0391	0.0286	0.0693	0.0639	0.0597	0.5039	0.4660	0.3599	0.5367	0.6300	0.4034
0.0514	0.0467	0.0297	0.0693	0.0694	0.0525	0.5016	0.4928	0.3457	0.5240	0.6435	0.3625
0.0496	0.0421	0.0302	0.0705	0.0678	0.0582	0.4909	0.4643	0.3511	0.5178	0.6303	0.3746
0.0481	0.0392	0.0285	0.0698	0.0668	0.0585	0.4906	0.4535	0.3470	0.5221	0.6263	0.3765
0.0487	0.0402	0.0288	0.0699	0.0652	0.0603	0.4985	0.4615	0.3587	0.5336	0.6237	0.4012
0.0506	0.0454	0.0298	0.0708	0.0700	0.0542	0.4900	0.4734	0.3468	0.5143	0.6386	0.3646
0.0510	0.0480	0.0292	0.0695	0.0699	0.0532	0.5037	0.4975	0.3556	0.5122	0.6519	0.3660
0.0508	0.0459	0.0295	0.0695	0.0692	0.0533	0.5106	0.5011	0.3604	0.5208	0.6455	0.3713
0.0487	0.0428	0.0278	0.0680	0.0669	0.0498	0.5041	0.4833	0.3545	0.5159	0.6389	0.3649

**Table C.13**

Average AUPR values for different settings of the parameter  $x$ , defining the percentage of stocks with the highest autocovariance (or standard deviation) used for the clustering procedure. Stock market: Europe. The table represents the average AUPR values obtained by varying the parameter  $x$  used to select the financial instruments (referring to the STOXX Europe 50) with the highest autocovariance in the case of  $I_t^{AC}$ , or standard deviation for  $I_t^{STD}$ . The parameter  $x$  varies from 100% to 40%. For the mixed case, we select the intersection of the stocks extracted by the previous settings (autocovariance and standard deviation). The first three columns refer to the –4% crisis scenario for  $I_t^{AC,STD}$ ,  $I_t^{AC}$  and  $I_t^{STD}$ , respectively. Columns four to six refer to the –4% crisis scenario and to the smoothed (SM) indicators. Columns seven to nine refer to the –3% scenario and the last three columns encompass the AUPR values of the smoothed (SM) indicators for the –3% crisis scenario.

4% Std + Ac	4% Ac	4% Std	4%-SM Std + Ac	4%-SM Ac	4%-SM Std	3% Std + Ac	3% Ac	3% Std	3%-SM Std + Ac	3%-SM Ac	3%-SM Std
0.0338	0.0265	0.0295	0.0471	0.0469	0.0431	0.4825	0.4261	0.3641	0.6581	0.6291	0.5175
0.0334	0.0257	0.0288	0.0473	0.0468	0.0430	0.4794	0.4182	0.3600	0.6557	0.6172	0.5018
0.0330	0.0245	0.0282	0.0466	0.0463	0.0417	0.4799	0.4119	0.3510	0.6565	0.6181	0.4835
0.0329	0.0269	0.0266	0.0477	0.0473	0.0405	0.4886	0.4397	0.3652	0.6697	0.6386	0.5412
0.0331	0.0258	0.0294	0.0464	0.0452	0.0434	0.4769	0.4186	0.3585	0.6567	0.6274	0.5223
0.0324	0.0238	0.0281	0.0458	0.0456	0.0421	0.4765	0.4081	0.3468	0.6534	0.6177	0.4794
0.0319	0.0223	0.0270	0.0454	0.0443	0.0406	0.4674	0.3875	0.3310	0.6512	0.6048	0.4578
0.0326	0.0260	0.0284	0.0468	0.0459	0.0422	0.4848	0.4305	0.3627	0.6595	0.6303	0.5386
0.0326	0.0252	0.0291	0.0457	0.0445	0.0431	0.4753	0.4139	0.3511	0.6524	0.6218	0.5054
0.0321	0.0237	0.0280	0.0457	0.0450	0.0419	0.4715	0.4038	0.3467	0.6508	0.6183	0.4809
0.0311	0.0215	0.0266	0.0438	0.0415	0.0395	0.4621	0.3775	0.3219	0.6442	0.5882	0.4509
0.0337	0.0275	0.0297	0.0468	0.0467	0.0430	0.4839	0.4256	0.3621	0.6582	0.6322	0.5253
0.0326	0.0244	0.0281	0.0456	0.0446	0.0420	0.4740	0.4097	0.3429	0.6466	0.6141	0.4834
0.0319	0.0232	0.0275	0.0449	0.0441	0.0410	0.4709	0.3980	0.3344	0.6447	0.6054	0.4647
0.0318	0.0227	0.0271	0.0444	0.0430	0.0399	0.4658	0.3860	0.3234	0.6472	0.5956	0.4543
0.0334	0.0273	0.0290	0.0466	0.0467	0.0432	0.4833	0.4229	0.3581	0.6483	0.6182	0.5078
0.0345	0.0289	0.0266	0.0486	0.0489	0.0406	0.4952	0.4503	0.3636	0.6794	0.6573	0.5445
0.0351	0.0284	0.0292	0.0479	0.0478	0.0437	0.4871	0.4398	0.3689	0.6667	0.6421	0.5361
0.0355	0.0288	0.0295	0.0481	0.0483	0.0437	0.4866	0.4362	0.3630	0.6644	0.6351	0.5169
0.0350	0.0277	0.0286	0.0478	0.0472	0.0420	0.4852	0.4269	0.3598	0.6622	0.6229	0.4969

**Table C.14**

Average AUPR values for different settings of the parameter  $x$ , defining the percentage of stocks with the highest autocovariance (standard deviation) used for the clustering procedure. Stock market: Asia/Pacific. The table represents the average AUPR values obtained by varying the parameter  $x$  used to select the financial instruments (referring to STOXX Asia/Pacific 600) with the highest autocovariance in the case of  $I_t^{AC}$ , or standard deviation for  $I_t^{STD}$ . The parameter  $x$  varies from 100% to 40%. For the mixed, case we select the intersection of the stocks extracted by the previous settings (autocovariance and standard deviation). The first three columns refer to the –4% crisis scenario for  $I_t^{AC,STD}$ ,  $I_t^{AC}$  and  $I_t^{STD}$ , respectively. Columns four to six refer to the –4% crisis scenario and to the smoothed (SM) indicators. Columns seven to nine refer to the –3% scenario and the last three columns encompass the AUPR values of the smoothed (SM) indicators for the –3% crisis scenario.

4% Std + Ac	4% Ac	4% Std	4%-SM Std + Ac	4%-SM Ac	4%-SM Std	3% Std + Ac	3% Ac	3% Std	3%-SM Std + Ac	3%-SM Ac	3%-SM Std
0.0167	0.0149	0.0129	0.0222	0.0220	0.0216	0.4379	0.4010	0.3470	0.5948	0.6001	0.5600
0.0168	0.0155	0.0127	0.0225	0.0218	0.0214	0.4403	0.4027	0.3494	0.5891	0.5944	0.5493
0.0167	0.0146	0.0127	0.0221	0.0219	0.0206	0.4317	0.3966	0.3353	0.5832	0.5939	0.5383
0.0176	0.0149	0.0145	0.0232	0.0224	0.0242	0.4612	0.4137	0.3799	0.6101	0.6060	0.5957
0.0162	0.0144	0.0119	0.0223	0.0220	0.0214	0.4492	0.4053	0.3504	0.5927	0.5969	0.5537
0.0170	0.0151	0.0128	0.0220	0.0218	0.0203	0.4388	0.4018	0.3351	0.5862	0.5949	0.5369
0.0160	0.0141	0.0120	0.0219	0.0219	0.0206	0.4333	0.3929	0.3287	0.5857	0.5933	0.5381
0.0175	0.0156	0.0133	0.0227	0.0220	0.0215	0.4540	0.4078	0.3704	0.5988	0.6011	0.5730
0.0165	0.0148	0.0133	0.0223	0.0218	0.0221	0.4384	0.3997	0.3412	0.5904	0.5975	0.5549
0.0167	0.0143	0.0123	0.0223	0.0216	0.0213	0.4302	0.3918	0.3326	0.5824	0.5903	0.5429
0.0169	0.0145	0.0129	0.0219	0.0218	0.0213	0.4187	0.3810	0.3131	0.5776	0.5869	0.5222
0.0172	0.0147	0.0135	0.0223	0.0218	0.0215	0.4575	0.4129	0.3725	0.6014	0.6033	0.5727
0.0174	0.0152	0.0142	0.0223	0.0216	0.0222	0.4388	0.4005	0.3411	0.5816	0.5904	0.5319
0.0159	0.0140	0.0120	0.0215	0.0215	0.0207	0.4252	0.3893	0.3291	0.5832	0.5919	0.5311
0.0160	0.0140	0.0119	0.0219	0.0217	0.0210	0.4241	0.3877	0.3199	0.5787	0.5918	0.5284
0.0166	0.0144	0.0131	0.0221	0.0214	0.0214	0.4530	0.4083	0.3662	0.5924	0.5990	0.5635
0.0181	0.0159	0.0151	0.0231	0.0225	0.0227	0.4725	0.4291	0.3880	0.6093	0.6080	0.5915
0.0180	0.0158	0.0137	0.0228	0.0225	0.0228	0.4536	0.4158	0.3541	0.6049	0.6083	0.5669
0.0175	0.0154	0.0133	0.0224	0.0219	0.0219	0.4445	0.4047	0.3492	0.5961	0.6013	0.5550
0.0169	0.0152	0.0127	0.0222	0.0219	0.0211	0.4418	0.4057	0.3469	0.5886	0.5934	0.5559

## Appendix D. Supplementary material

Supplementary data associated with this article can be found, in the online version, at <https://doi.org/10.1016/j.jbusres.2019.10.043>.

## References

- Ahrweiler, P., Gilbert, N., & Pyka, A. (2016). *Joining complexity science and social simulation for innovation policy: Agent-based modelling using the SKIN platform*. Cambridge: Scholars Publishing.
- Alessi, L., & Detken, C. (2011). Quasi real time early warning indicators for costly asset price boom/bust cycles: A role for global liquidity. *European Journal of Political Economy*, 27(3), 520–533.
- Andreou, E., & Ghysels, E. (2009). Structural breaks in financial time series. In *Handbook of financial time series* (pp. 839–870). Springer.
- Ausloos, M., Ivanova, K., & Vandewalle, N. (2002). Crashes: symptoms, diagnoses and remedies. In *Empirical science of financial fluctuations* (pp. 62–76). Springer.
- Ausloos, M., Jovanovic, F., & Schinckus, C. (2016). On the usual misunderstandings between econophysics and finance: Some clarifications on modelling approaches and efficient market hypothesis. *International Review of Financial Analysis*, 47, 7–14.
- Baillie, R. T., & Bollerslev, T. (1994). Cointegration, fractional cointegration, and exchange rate dynamics. *The Journal of Finance*, 49(2), 737–745.
- Bank for International Settlements (2012). Operationalising the selection and application of macroprudential instruments. Number 48 in CGFS Papers. BIS.
- Bao, T., Hennequin, M., Hommes, C., et al. (2019). Coordination on bubbles in large-group asset pricing experiments. *Journal of Economic Dynamics & Control*. <https://doi.org/10.1016/j.jedc.2019.05.001>.
- Barberis, N., Shleifer, A., & Wurgler, J. (2005). Comovement. *Journal of Financial Economics*, 75(2), 283–317.
- Berge, T. J., & Jorda, Ò. (2011). Evaluating the classification of economic activity into recessions and expansions. *American Economic Journal: Macroeconomics*, 3(2), 246–277.
- Bethke, S., Gehde-Trapp, M., & Kempf, A. (2017). Investor sentiment, flight-to-quality, and corporate bond comovement. *Journal of Banking & Finance*, 82, 112–132.
- Borgatti, S. P., & Halgin, D. S. (2011). On network theory. *Organization Science*, 22(5), 1168–1181.
- Brenner, R. J., & Kroner, K. F. (1995). Arbitrage, cointegration, and testing the unbiasedness hypothesis in financial markets. *Journal of Financial and Quantitative Analysis*, 30(1), 23–42.
- Caldara, D., & Iacoviello, M. (2018). Measuring geopolitical risk. FRB International Finance Discussion Paper, (1222).
- Carpenter, M. A., Li, M., & Jiang, H. (2012). Social network research in organizational contexts: A systematic review of methodological issues and choices. *Journal of Management*, 38(4), 1328–1361.
- Chen, L., Liu, R., Liu, Z.-P., Li, M., & Aihara, K. (2012). Detecting early-warning signals for sudden deterioration of complex diseases by dynamical network biomarkers. *Scientific Reports*, 2, 342.
- Dakos, V., Carpenter, S. R., Brock, W. A., Ellison, A. M., Guttal, V., Ives, A. R., ... Scheffer, M. (2012). Methods for detecting early warnings of critical transitions in time series illustrated using simulated ecological data. *PLoS One*, 7(7), e41010.
- Flori, A., Pammolli, F., Bulyrev, S. V., Regis, L., & Stanley, H. E. (2019). Communities and regularities in the behavior of investment fund managers. *Proceedings of the National Academy of Sciences*, 116(14), 6569–6574.
- Forbes, K. J., & Chinn, M. D. (2004). A decomposition of global linkages in financial markets over time. *Review of Economics and Statistics*, 86(3), 705–722.
- Forbes, K. J., & Rigobon, R. (2002). No contagion, only interdependence: measuring stock market comovements. *The Journal of Finance*, 57(5), 2223–2261.
- Gkillas, K., Tsagkaros, A., & Vortelinos, D. I. (2019). Integration and risk contagion in financial crises: Evidence from international stock markets. *Journal of Business Research*, 104, 350–365.
- Hausman, A., & Johnston, W. J. (2014). The role of innovation in driving the economy: Lessons from the global financial crisis. *Journal of Business Research*, 67(1), 2720–2726.
- Hirschleifer, D., & Hong Teoh, S. (2003). Herd behaviour and cascading in capital markets: A review and synthesis. *European Financial Management*, 9(1), 25–66.
- Hommes, C. (2013). *Behavioral rationality and heterogeneous expectations in complex economic systems*. Cambridge University Press.
- Hommes, C., Sonnemans, J., Tuinstra, J., & Van de Velden, H. (2004). Coordination of expectations in asset pricing experiments. *The Review of Financial Studies*, 18(3), 955–980.
- Hommes, C., Sonnemans, J., Tuinstra, J., & Van de Velden, H. (2008). Expectations and bubbles in asset pricing experiments. *Journal of Economic Behavior & Organization*, 67 (1), 116–133.
- Hong, H., & Stein, J. C. (2003). Differences of opinion, short-sales constraints, and market crashes. *The Review of Financial Studies*, 16(2), 487–525.
- Huber, T. A., & Sornette, D. (2016). Can there be a physics of financial markets? methodological reflections on econophysics. *The European Physical Journal Special Topics*, 225(17–18), 3187–3210.
- Hüsler, A., Sornette, D., & Hommes, C. H. (2013). Super-exponential bubbles in lab experiments: Evidence for anchoring over-optimistic expectations on price. *Journal of Economic Behavior & Organization*, 92, 304–316.
- Hwang, S., & Salmon, M. (2004). Market stress and herding. *Journal of Empirical Finance*, 11(4), 585–616.
- Kacperczyk, M., & Schnabl, P. (2010). When safe proved risky: Commercial paper during the financial crisis of 2007–2009. *Journal of Economic Perspectives*, 24(1), 29–50.
- Kaminsky, G. L., & Reinhart, C. M. (1999). The twin crises: The causes of banking and balance-of-payments problems. *American Economic Review*, 89(3), 473–500.
- Khandani, A. E., Kim, A. J., & Lo, A. W. (2010). Consumer credit-risk models via machine-learning algorithms. *Journal of Banking & Finance*, 34(11), 2767–2787.
- Kirman, A. (2010). *Complex economics: Individual and collective rationality*. London: Routledge.
- Kuester, K., Mittnik, S., & Paoletti, M. S. (2006). Value-at-risk prediction: A comparison of alternative strategies. *Journal of Financial Econometrics*, 4(1), 53–89.
- Kutner, R., Ausloos, M., Grech, D., Di Matteo, T., Schinckus, C., & Stanley, H. E. (2018). Econophysics and sociophysics: Their milestones & challenges. *Physica A: Statistical Mechanics and its Applications*, 516, 240–253.
- Lenton, T., Livina, V., Dakos, V., Van Nes, E., & Scheffer, M. (2012). Early warning of climate tipping points from critical slowing down: Comparing methods to improve robustness. *Philosophical Transactions of the Royal Society A: Mathematical, Physical and Engineering Sciences*, 370(1962), 1185–1204.
- Liu, R., Chen, P., Aihara, K., & Chen, L. (2015). Identifying early-warning signals of critical transitions with strong noise by dynamical network markers. *Scientific Reports*, 5, 17501.
- Li, M., Zeng, T., Liu, R., & Chen, L. (2013). Detecting tissue-specific early warning signals for complex diseases based on dynamical network biomarkers: Study of type 2 diabetes by cross-tissue analysis. *Briefings in Bioinformatics*, 15(2), 229–243.
- Lusted, L. B. (1960). Logical analysis in roentgen diagnosis: Memorial fund lecture. *Radiology*, 74(2), 178–193.
- Lux, T. (1995). Herd behaviour, bubbles and crashes. *The Economic Journal*, 105(431), 881–896.
- Lux, T. (1998). The socio-economic dynamics of speculative markets: Interacting agents, chaos, and the fat tails of return distributions. *Journal of Economic Behavior & Organization*, 33(2), 143–165.
- Mantegna, R. N., & Stanley, H. E. (1999). *Introduction to econophysics: Correlations and complexity in finance*. Cambridge University Press.
- Moon, H., & Lu, T.-C. (2015). Network catastrophe: Self-organized patterns reveal both the instability and the structure of complex networks. *Scientific Reports*, 5, 9450.
- Newman, M. E. (2003). The structure and function of complex networks. *SIAM Review*, 45(2), 167–256.
- Orsenigo, L., Pammolli, F., & Riccaboni, M. (2001). Technological change and network dynamics: Lessons from the pharmaceutical industry. *Research Policy*, 30(3), 485–508.
- Oya, S., Aihara, K., & Hirata, Y. (2014). Forecasting abrupt changes in foreign exchange markets: Method using dynamical network marker. *New Journal of Physics*, 16(11), 115015.
- Pammolli, F., & Riccaboni, M. (2002). Technological regimes and the growth of networks: An empirical analysis. *Small Business Economics*, 19(3), 205–215.
- Peterson, W. W., & Birdsall, T. G. (1953). *The theory of signal detectability. Part 1: the general theory. Technical report*. Michigan University Ann Arbor Engineering Research Institute.
- Plerou, V., Gopikrishnan, P., Rosenow, B., Amaral, L. A., & Stanley, H. E. (2000). Econophysics: Financial time series from a statistical physics point of view. *Physica A: Statistical Mechanics and its Applications*, 279(1–4), 443–456.
- Preis, T., Moat, H. S., & Stanley, H. E. (2013). Quantifying trading behavior in financial markets using google trends. *Scientific Reports*, 3, 1684.
- Preis, T., Schneider, J. J., & Stanley, H. E. (2011). Switching processes in financial markets. *Proceedings of the National Academy of Sciences*, 108(19), 7674–7678.
- Provost, F., & Kohavi, R. (1998). Glossary of terms. *Journal of Machine Learning*, 30(2–3), 271–274.
- Pyka, A., & Scharnhorst, A. (2009). *Innovation networks: New approaches in modelling and analyzing*. Springer Science & Business Media.
- Riccaboni, M., & Pammolli, F. (2003). Technological regimes and the evolution of networks of innovators. Lessons from biotechnology and pharmaceuticals. In *Applied Evolutionary Economics* (Vol. 2)Edward Elgar Publishing.
- Rösch, C. G., & Kaserer, C. (2013). Market liquidity in the financial crisis: The role of liquidity commonality and flight-to-quality. *Journal of Banking & Finance*, 37(7), 2284–2302.
- Rosser, J. B. (1999). On the complexities of complex economic dynamics. *Journal of Economic Perspectives*, 13(4), 169–192.
- Roundy, P. T., Bradshaw, M., & Brockman, B. K. (2018). The emergence of entrepreneurial ecosystems: A complex adaptive systems approach. *Journal of Business Research*, 86, 1–10.
- Sarin, P. (2013). On policymakers' loss functions and the evaluation of early warning systems. *Economics Letters*, 119(1), 1–7.
- Scheffer, M., Bascompte, J., Brock, W. A., Brovkin, V., Carpenter, S. R., Dakos, V., ... Sugihara, G. (2009). Early-warning signals for critical transitions. *Nature*, 461(7260), 53.
- Scheffer, M., Carpenter, S. R., Lenton, T. M., Bascompte, J., Brock, W., Dakos, V., ... Pascual, M. (2012). Anticipating critical transitions. *Science*, 338(6105), 344–348.
- Schweitzer, F., Fagiolo, G., Sornette, D., Vega-Redondo, F., Vespignani, A., & White, D. R. (2009). Economic networks: The new challenges. *Science*, 325(5939), 422–425.
- Shiller, R. J., & Pound, J. (1989). Survey evidence on diffusion of interest and information among investors. *Journal of Economic Behavior & Organization*, 12(1), 47–66.
- Slotte-Kock, S., & Coville, N. (2010). Entrepreneurship research on network processes: A review and ways forward. *Entrepreneurship Theory and Practice*, 34(1), 31–57.
- Sornette, D. (2002). Predictability of catastrophic events: Material rupture, earthquakes, turbulence, financial crashes, and human birth. *Proceedings of the National Academy of Sciences*, 99(suppl 1), 2522–2529.
- Sornette, D. (2003). Critical market crashes. *Physics Reports*, 378(1), 1–98.
- Sornette, D. (2017). *Why stock markets crash: Critical events in complex financial systems* (Vol. 49). Princeton, New Jersey: Princeton University Press.
- Spackman, K. A. (1989). Signal detection theory: Valuable tools for evaluating inductive learning. In *Proceedings of the sixth international workshop on Machine learning* (pp. 160–163). Elsevier.

- Spelta, A., Pecora, N., Flori, A., & Pammolli, F. (2018b). Transition drivers and crisis signaling in stock markets. Technical Report MPRA 88127. Germany: University Library of Munich.
- Spelta, A. (2017). Financial market predictability with tensor decomposition and links forecast. *Applied Network Science*, 2(1), 7.**
- Spelta, A., Flori, A., & Pammolli, F. (2018). Investment communities: Behavioral attitudes and economic dynamics. *Social Networks*, 55, 170–188.
- Spelta, A., Pecora, N., & Kaltwasser, P. R. (2019). Identifying systemically important banks: A temporal approach for macroprudential policies. *Journal of Policy Modeling*, 41(1), 197–218.
- Swets, J. A. (1973). The relative operating characteristic in psychology: a technique for isolating effects of response bias finds wide use in the study of perception and cognition. *Science*, 182(4116), 990–1000.
- Takayasu, M., Watanabe, T., & Takayasu, H. (2010). Econophysics approaches to large-scale business data and financial crisis. In *proceedings of Tokyo Tech-Hitotsubashi interdisciplinary conference APFA7*. Springer Science & Business Media.
- Vasconcelos, F. C., & Ramirez, R. (2011). Complexity in business environments. *Journal of Business Research*, 64(3), 236–241.
- Wang, X. F., & Chen, G. (2003). Complex networks: Small-world, scale-free and beyond. *IEEE Circuits and Systems Magazine*, 3(1), 6–20.
- Zhao, L., Yang, G., Wang, W., Chen, Y., Huang, J., Ohashi, H., & Stanley, H. E. (2011). Herd behavior in a complex adaptive system. *Proceedings of the National Academy of Sciences*, 108(37), 15058–15063.

**Alessandro Spelta**, after obtaining the Master Degree in Economics at the University of Pavia, he started his PhD in Economics. During the Ph.D. (2010–2014), he produced papers applying computational models to economics and finance. In 2014, he started his first PostDoc at the Catholic University of Milan working on two European projects on Early Warning Crisis for financial crisis: MACFINROBODS, Integrated Macro Financial Modeling for Robust Policy Design and RAstaNEWS, Macro-Risk Assessment and Stabilization Policies with New Early Warning Signals. Between 2016 and 2017, he worked as Big Data Analyst at OMNICOM MEDIA GROUP where he was involved in the development of Marketing Analytic Models that supports marketers to create data-driven marketing plans, specifically geared towards achieving business goals. From 2016 to 2017, he was Post Doctoral researcher in Statistics at the University of Pavia. Here he focused on the development of a novel distress measure for banking systems. In 2018, he has been involved in the research project of the Center for Analysis Decisions and Society of Human

Technopole and from January 2019 he is Assistant Professor in statistics at the University of Pavia.

**Andrea Flori** is Assistant Professor at the Department of Management, Economics and Industrial Engineering of Polytechnic of Milan. His main research interests cover the application of econometric and network theory approaches to the study of financial stability, systemic risk and the emergence of interdependences in economic and financial systems. He has published in several international peer-reviewed journals in finance and physics. He holds a BSc in Economics of Financial Markets (University of Siena), a MSc in Finance (University of Siena) and a Ph.D. in Economics (IMT, School for Advanced Studies Lucca).

**Nicolò Pecora** is Assistant Professor in the Department of Economics and Social Sciences in the Catholic University of Piacenza, where formerly he was post-doctoral fellow. He received his Ph.D. in Quantitative Methods for Economic Policy in the Catholic University of Milano. He has been involved in the European project MACFINROBODS, Integrated Macro Financial Modeling for Robust Policy Design. His current research interests include nonlinear economic dynamics, bifurcation theory, economic complexity and financial networks. He has published papers in journals such as *Journal of Economic Behavior and Organization*, *Journal of Economic Dynamics and Control*, *Macroeconomic Dynamics*, *Journal of Money, Credit and Banking*, *Chaos* among others.

**Fabio Pammolli** is Full Professor of Economics and Management at the Politecnico di Milano, where he serves as a member of the scientific board of the Ph.D. in Data Analytics and Decision Sciences. His research combines different methodologies to cover topics in the economics of pharmaceuticals, health and pensions, management analytics and in the analysis of growth, diversification, and instability of multiproduct firms. He was a visiting scientist at leading universities such as Sciences Po, the London School of Economics, Harvard University, Massachusetts Institute of Technology, Boston University, Northeastern University. His research has been published in leading academic journals, including *Science*, *PNAS*, *Nature Drug Discovery*, *Nature Physics*, *Annals of Operation Research*, *Science Advances*, *Management Science*, *European Journal of Health Economics*, *Health Affairs*, *Journal of Evolutionary Economics*. Since 2015, he is a member of the Investment Committee of the European Fund for Strategic Investments at the European Investment Bank, Luxembourg.